Distributed Interference Management: A Broadcast Approach

Maha Zohdy, Ali Tajer, *Senior Member, IEEE*, and Shlomo Shamai, *Life Fellow, IEEE*

***Abstract*— Effective interference management in the multiuser interference channel strongly hinges on the channel state information's availability at the transmitters (CSIT). In a broad range of emerging large-scale and distributed networks (e.g., the Internet of Things), acquiring the CSIT is prohibitive due to the extensive information exchange that it imposes. As a result, the interference management approaches that rely on the CSIT lose their effectiveness in such circumstances. This article focuses on the two-user interference channel and proposes a *broadcast approach* to interference management. Its hallmark is that the transmitters, unlike the receivers, are entirely oblivious to instantaneous channel states. Each transmitter splits its message into multiple superimposed encoded information layers, where each layer is adapted to a given possible state for the combined states of all channels. Depending on the relative gain between the direct and interfering channels, each receiver opportunistically decodes a subset of both transmitters' received layers. An average achievable rate region is delineated, serving as an inner bound on the Gaussian interference channel's average capacity region in the absence of CSIT. Finally, an upper bound on the gap between the achievable sum-rate and the sum-rate capacity is established.**

***Index Terms*— Broadcast, distributed, capacity region, interference.**

I. Introduction

THE multiuser interference channel constitutes a canonical building block in interference-limited wireless networks in which multiple transmitters communicate with their designated receivers while interfering with others. Designing and analyzing interference management schemes has a rich literature. Irrespective of their discrepancies, the existing approaches often rely on the accurate availability of the channel state information at the transmitters (CSIT) and the receivers. While acquiring such information at the receiver can be facilitated through training sessions, acquiring it at the transmitters necessitates each receiver reporting it to all transmitters. Such additional information exchange incurs high communication costs and latency, especially when the network size grows.

Under the assumption of perfect availability of CSIT at all transmitters, there exists rich literature on characterizing the capacity region. Representative known results in the asymptote of high signal-to-noise ratio (SNR) regime include the degrees-of-freedom (DoF) region achievable by interference alignment [1], [2]. In the non-asymptotic SNR regime of particular note is the achievable rate region due to Han-Kobayashi (HK) [3], [4], which is shown to achieve rates within one bit of the capacity region for the Gaussian interference channel [5]. While unknown in its general form, the capacity region is known in special cases, including the strong interference channel [6], [7], the discrete additive degraded interference channel [8], and certain classes of the deterministic interference channel [9]–[12]. There are extensive studies on circumventing the challenges associated with analyzing optimal resource allocation over the HK region [13]–[20].

Interference management without CSIT has also been the subject of intense studies more recently, with more focus on the high SNR regime. Representative studies in the high SNR regime include characterizing the DoF region for the two-user multi-antenna interference channel in [21]–[27]; compound interference networks in [28]; blind interference alignment in [29]–[38]; opportunistic blind interference alignment in [39]; interference management via leveraging network topologies in [40] and [41]; and ergodic interference channels in [42]–[44]. In the non-asymptotic SNR regime, the studies are more limited, and they include analysis on the capacity region of the erasure interference channel in [45] and [46]; the compound interference channel in [47]; ergodic capacity for the Z-interference channel in [48]; ergodic capacity of the strong and very strong interference channels in [49] and [50]; and approximate capacity region for the fast-fading channels in [51] and [52].

In this article, conductive to relieving dependency on full CSIT, we focus on the two-user and finite-state Gaussian interference channel, in which the channel state information is unknown to the transmitters, while known to the receivers. We characterize an inner bound on the capacity region of this channel in the non-asymptotic SNR regime. Our focus is distinct from those on the high SNR regime (c.f. [21]–[43]) and those on the special cases in the non-asymptotic SNR regime, e.g., erasure, compound, Z, and ergodic channels (c.f. [45]–[52]). We remark that among the existing studies, the most relevant studies include [47], which considers the

Manuscript received April 14, 2020; revised August 17, 2020 and September 18, 2020; accepted September 19, 2020. Date of publication September 24, 2020; date of current version January 15, 2021. The work of M. Zohdy and A. Tajer has been supported in part by the U. S. National Science Foundation grant ECCS-1933107. The work of S. Shamai was supported by the WIN consortium via the Israel minister of economy and science. The associate editor coordinating the review of this article and approving it for publication was S. Bhashyam. *(Corresponding author: Ali Tajer.)*

Maha Zohdy and Ali Tajer are with the Department of Electrical, Computer, and Systems Engineering, Rensselaer Polytechnic Institute, Troy, NY 12180 USA (e-mail: tajer@ecse.rpi.edu).

Shlomo Shamai is with the Department of Electrical Engineering, Technion-Israel Institute of Technology, Haifa 3200003, Israel.

Color versions of one or more of the figures in this article are available online at https://ieeexplore.ieee.org.

Digital Object Identifier 10.1109/TCOMM.2020.3026386

0090-6778 © 2020 IEEE. Personal use is permitted, but republication/redistribution requires IEEE permission.
See https://www.ieee.org/publications/rights/index.html for more information.

Authorized licensed use limited to: The Libraries at Rensselaer Polytechnic Institute. Downloaded on September 12,2022 at 21:48:32 UTC from IEEE Xplore. Restrictions apply.

compound interference channel without the CSIT as well as [39], which proposes an opportunistic blind interference alignment scheme in the general K-user interference channel. Both approaches consider the multi-layer transmission. Our main distinction from the study in [47] is that we dispense with the degradedness assumption, i.e., we assume that the randomly varying states of interfering channels do not necessarily exhibit degradedness. Furthermore, our approach is also distinct from [39] in the way that the information layers are generated and adapted to the channel. Specifically, in our finite-state channels, we generate a set of information layers adapted to each possible channel state, while in [39], the channels are generated independently of the channel states. Besides these, there is also a distinction in the channel model (finite-state versus continuous fading), and the analysis (general SNR versus high SNR in [39]).

For characterizing an inner bound, we propose a distributed interference management approach based on a multi-layer superposition coding known as the broadcast approach [53], [54]. In the absence of the CSIT, designing an effective superposition coding scheme at each transmitter relies on considering all possible interference levels caused by such transmitter and the interfering levels observed by its designated receiver from other users. The broadcast approach, initially proposed for the compound broadcast channel [53], is an effective approach to circumventing lack of the CSIT. Based on that, a broadcast strategy was introduced in [54] and [55] for the slowly-fading single-user channel. In the broadcast approach, a transmitter that is oblivious to the channel linking it to its designated receiver performs superposition coding by splitting its data stream into several independently-generated coded layers with different rates. The rate of each layer is adapted to a specific channel state. The transmitter then superimposes and transmits all the generated layers, and the receiver decodes as many layers as the actual quality of the channel affords. Other relevant studies on the single-user fading channels with superposition coding (rate-splitting) include [19], [56]–[60]. This approach is then studied under various assumptions for multiple access communications [61]–[66], and for interference channels in [18]–[20]. Specifically, the studies in [18] and [20] adopt superposition coding for opportunistic transmission and decoding of interference and provide the analysis in the high-SNR regime. The study in [19] investigates opportunistic decoding of the interference, with the emphasis on the decoding complexity and outage analysis.

Distinct from the studies above, in this article, we focus on the non-asymptotic regime and characterize an achievable rate region. Besides the inner bound, we analytically quantify an upper bound on the gap between the achievable and sum-rate and the sum-rate capacity. Our primary focus in the analysis is on the two-user finite-state Gaussian channel, for which case we provide the rate regions and the gap analysis. We also provide a generalization of the proposed encoding schemes to the N-user finite-state Gaussian channel.

II. Channel Model

Consider the two-user slowly-fading Gaussian interference channel, in which the coefficient of the channel connecting transmitter i to receiver j is denoted by h_{ij}^* for $i,j \in \{1,2\}$. We refer to h_{ii}^* and h_{ij}^* as the *direct* and *cross* channel coefficients, respectively, $\forall\ i \neq j$. The signal received by receiver i is denoted by

$$y_i^* = h_{ii}^*\, x_i^* \ +\ h_{ij}^*\, x_j^* \ +\ n_i^*, \tag{1}$$

where x_i^* denotes the signal transmitted by transmitter i, and n_i^* accounts for the additive white Gaussian noise distributed according to $\mathcal{N}(0, N_i)$. The transmitted symbol x_i^* is subject to the average power constraint P_i^*, i.e., $\mathbb{E}[x_i^*] \leq P_i^*$. Each channel is assumed to follow a block fading model in which the channel coefficients remain constant for the duration of a transmission block of length n, and randomly change to another state afterward. We consider an ℓ-state channel model in which each channel coefficient randomly and independently of the rest of the channels takes one of the ℓ possible states $\{\alpha_i : i \in \{1,\ldots,\ell\}\}$. Without loss of generality, we assume that $0 < \alpha_1 < \cdots < \alpha_\ell < +\infty$. The ℓ-state interference channel in (1) gives rise to an interference channel with ℓ^2 different states. The entire channel states are assumed to be fully known to the receivers while being unknown to the transmitters. A statistically equivalent form of the ℓ-state interference channel in (1) is the standard interference channel model given by [67] and [68]

$$y_1 = x_1 \ +\ \sqrt{a_1} x_2 \ +\ n_1, \tag{2}$$

$$y_2 = \sqrt{a_2} x_1 \ +\ x_2 \ +\ n_2, \tag{3}$$

and the inputs satisfy $\mathbb{E}[x_i] \leq P_i$, where we have defined

$$a_1 \triangleq \left(\frac{h_{12}^*}{h_{22}^*}\right)^2 \frac{N_2}{N_1},\ a_2 \triangleq \left(\frac{h_{21}^*}{h_{11}^*}\right)^2 \frac{N_1}{N_2},\ P_i \triangleq \frac{(h_{ii}^*)^2}{N_i} P_i^*, \tag{4}$$

and the terms n_1 and n_2 are the additive noise terms distributed according to $\mathcal{N}(0,1)$. The equivalence between (1) and (2) can be established by setting

$$y_i \triangleq \frac{y_i^*}{\sqrt{N_i}}, \quad x_i \triangleq \frac{h_{ii}^*}{\sqrt{N_i}}\, x_i^*, \quad n_i \triangleq \frac{n_i^*}{\sqrt{N_i}}. \tag{5}$$

Channel gains a_1 and a_2 are statistically independent, inheriting their independence from that of the channel coefficients. By invoking the normalization in (4), it can be readily verified that the *cross* channel gains a_i take one of $K \triangleq \ell(\ell-1)+1$ possible states, which we denote by $\{\beta_1,\ldots,\beta_K\}$. Without loss of generality we assume they are in the ascending order. For the two-state channel, the *cross* channel gain takes one of the three states $\beta_1 \triangleq \frac{\alpha_1}{\alpha_2}, \beta_2 \triangleq 1$, and $\beta_3 \triangleq \frac{1}{\beta_1}$. Hence, the state of the network is specified by two cross links, rendering K^2 states for the network. We say that the network is in the state (β_s, β_t) when $(a_1, a_2) = (\beta_s, \beta_t)$. To distinguish different states, in state (β_s, β_t), we denote the outputs by

$$y_1^s = x_1 \ +\ \sqrt{\beta_s}\, x_2 \ +\ n_1, \tag{6}$$

$$y_2^t = \sqrt{\beta_t}\, x_1 \ +\ x_2 \ +\ n_2. \tag{7}$$

Hence, this interference channel can be equivalently presented as a network with two transmitters and K^2 receiver pairs, where each receiver pair corresponds to one possible channel state. In the case of *symmetric* interference channel, we have $a_1 = a_2$, and the number of possible channel combinations

Authorized licensed use limited to: The Libraries at Rensselaer Polytechnic Institute. Downloaded on September 12,2022 at 21:48:32 UTC from IEEE Xplore. Restrictions apply.

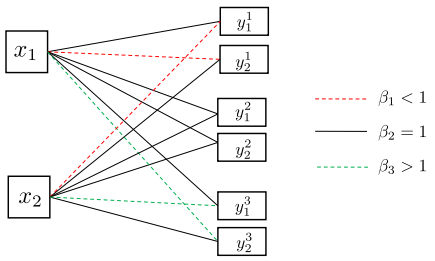

Fig. 1. Equivalent network for the symmetric channel.

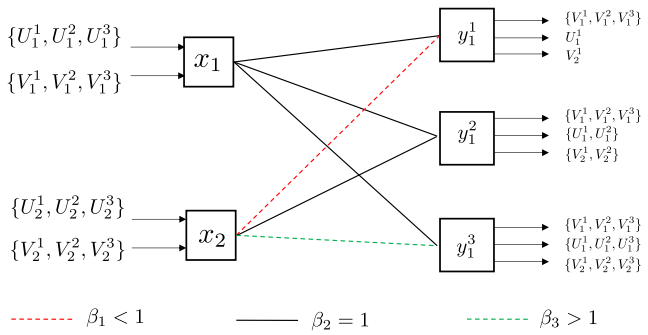

Fig. 2. Codebook assignments at transmitter 1 in the two-state channel.

reduces to K, rending an equivalent network with two transmitters and $2K$ receivers. Figure 1 depicts such a symmetric network for the two-state channel. Finally, we define

$$q_1^s \triangleq \mathbb{P}(a_1 = \beta_s) \quad \text{and} \quad q_2^s \triangleq \mathbb{P}(a_2 = \beta_s). \tag{8}$$

We use the notation $C(x, y) \triangleq \frac{1}{2}\log_2(1 + \frac{x}{1+y})$.

III. Rate-Splitting and Decoding Scheme

A. Background: Adapting Streams to the Single-User Channel

In order to motivate the proposed approach, we start by reviewing the broadcast strategy concept for a single-user channel introduced in [54]. When facing a two-state channel, the broadcast approach splits the transmitter's information stream into two streams, each corresponding to one fading state, and encodes them independently. The two encoded information streams are subsequently superimposed and transmitted over the channel. One of the streams, denoted by W_1, is always decoded by the receiver, while the second stream, denoted by W_2, is decoded only when the channel is *strong*.

Devising an effective broadcast approach for the Gaussian interference channel hinges on adapting the number of encoded information layers at each transmitter, distributing the total transmission power across the encoded layers, and effectively decoding the received layers at each receiver. We propose a novel broadcast approach in which information layers are adapted to the network state as a whole. In the remainder of this section, we discuss the layering and decoding schemes. In Section IV, we characterize an inner bound on the average capacity region. Furthermore, we quantify the gap between the achievable and capacity sum-rates and assess its scaling behavior with respect to the channel gains in the high SNR regime. This observation indicates that the proposed layering policy is effective in circumventing the uncertainty about the network state at the transmitters.

B. Adapting Streams to the Interference Channel

Each transmitter has two opposing effects on its designated and non-designated receivers. Hence, each transmitter splits its stream into multiple information layers, each adapted to one combined state of the network, and intended to be decoded by specific receivers. The rate of each layer is adapted to a particular network state, such that under the associated network state, the layer is decodable by the designated receiver.

In the broadcast approach, each transmitter and the K^2 receivers can be viewed as forming a multiple access channel, in which each receiver aims to decode as many information layers as possible that are transmitted by both transmitters. Hence, the multiuser network model in (6) is equivalent to a collection of multiple access channels. A key feature of these multiple access channels is that for $s < k$, the multiple access channel at receiver y_i^s is degraded with respect to the channel at y_i^k. Therefore, receiver y_i^k can successfully decode all the layers adapted to the channels with the designated receivers $\{y_i^1, \ldots, y_i^s\}$. At receiver y_i^k, every layer decoded form transmitter i directly increases the achievable rate, whereas every layer decoded from the other transmitter indirectly increases the achievable rate by canceling a part of the interfering signal. Based on these observations, transmitter i splits its message into $2K$ layers denoted by $\{V_i^k, U_i^k\}_{k=1}^K$, each serving a specific purpose. Specifically, by noting that in the standard model in (6), the direct channels gains are constant, and only the cross channels' states vary. Hence, each of these $2K$ layers is designated to a specific *cross* channel state and receiver.

- Transmitter 1 (or 2) adapts layer V_1^k (or V_2^k) to the state of the channel linking transmitter 1 (or 2) to the *unintended* receiver y_2^k (or y_1^k): while the intended receivers $\{y_1^k\}_{k=1}^K$ (or $\{y_2^k\}_{k=1}^K$) will be decoding all codebooks $\{V_1^k\}_{k=1}^K$ (or $\{V_2^k\}_{k=1}^K$), the non-intended receivers $\{y_2^k\}_{k=1}^K$ (or $\{y_1^k\}_{k=1}^K$) decode a subset of these codebooks depending on their channel strengths. More specifically, the non-intended receiver y_2^k (or y_1^k) decodes only the codebooks $\{V_1^s\}_{s=1}^k$ (or $\{V_2^s\}_{s=1}^k$).
- Transmitter 1 (or 2) adapts the layer U_1^k (or U_2^k) to the state of the channel linking transmitter 2 (or 1) to the *intended* receiver y_1^k (or y_2^k): while the unintended receivers $\{y_2^k\}_{k=1}^K$ (or $\{y_1^k\}_{k=1}^K$) will *not* be decoding any of the codebooks $\{U_1^k\}_{k=1}^K$ (or $\{U_2^k\}_{k=1}^K$), the intended receivers $\{y_1^k\}_{k=1}^K$ (or $\{y_2^k\}_{k=1}^K$) decode a subset of these codebooks depending on their channel strengths. More specifically, the intended receiver y_1^k (or y_2^k) decodes only the codebooks $\{U_1^s\}_{s=1}^k$ (or $\{U_2^s\}_{s=1}^k$).

Figure 2 focuses on the two-state channel ($\ell = 2$), and depicts the assignments of the codebooks to transmitter 1 and the set of codebooks decoded by each of the three receivers $\{y_1^k\}_{k=1}^3$ corresponding to transmitter 1.

We remark that the proposed layering approach is a generalization of that proposed for the compound interference

Authorized licensed use limited to: The Libraries at Rensselaer Polytechnic Institute. Downloaded on September 12,2022 at 21:48:32 UTC from IEEE Xplore. Restrictions apply.

TABLE I
SUCCESSIVE DECODING ORDER AT THE RECEIVERS

Receiver	Stage 1	Stage 2	Stage 3	Stage 4	Stage 5	Stage 6	Stage 7	Stage 8	Stage 9
y_i^1	V_i^1	V_j^1	V_i^2	V_i^3	U_i^1				
y_i^2	V_i^1	V_j^1	V_i^2	V_j^2	V_i^3	U_i^1	U_i^2		
y_i^3	V_j^1	V_i^1	V_j^2	V_i^2	V_j^3	V_i^3	U_i^1	U_i^2	U_i^3

channel [47]. In particular, the set of layers adapted to the *unintended* channel, $\{V_i^k\}$, has the same number of layers as those proposed by the scheme in [47]. On the other hand, the set $\{U_i^k\}$, which is adapted to the *intended* receiver, is a larger set. Hence, by adopting the appropriate power allocation among all layers, the layering scheme in [47] can be recovered. It is noteworthy that the study in [47] additionally also investigates the discrete memoryless channel.

C. Successive Decoding: Two-State Channel

In this subsection, we outline an *opportunistic* successive decoding strategy, which specifies the set and order of the codebooks decoded in each network state. In the proposed decoding scheme, each codebook will be decoded by multiple receivers. Hence, each codebook rate will be constrained by its associated most *degraded* channel state. Furthermore, any undecoded layer at a particular receiver imposes interference, which degrades the receiver's achievable rate. Hence, we devise a simple *opportunistic* successive decoding scheme. This scheme, specifically, determines (i) the set of receivers at which each codebook is decoded, and (ii) the order by which the codebooks are decoded successively at each receiver.

To formalize the decoding strategy, we define $\mathcal{V}_i^k$ as the set of receivers that decode the codebook V_i^k, and define $\mathcal{U}_i^k$ as the set of the receivers that decode U_i^k. Note that transmitter i adapts layers $\{V_i^k\}_{k=1}^3$ as baseline layers for the *intended* receivers $\{y_i^k\}_{k=1}^3$, as well as layers to be decoded by the set of *unintended* receivers $\{y_j^k\}_{k=1}^3$ for $j \neq i$, opportunistically. Hence, the sets $\mathcal{V}_i^k$, are given by

$$\mathcal{V}_1^k = \{y_1^s\}_{s=1}^3 \cup \{y_2^s\}_{s=k}^3 \quad \text{and} \quad \mathcal{V}_2^k = \{y_2^s\}_{s=1}^3 \cup \{y_1^s\}_{s=k}^3. \tag{9}$$

On the other hand, transmitter i adapts the layers $\{U_i^k\}_{k=1}^3$ only to the *intended* receivers $\{y_i^k\}_{k=1}^3$. Hence,

$$\mathcal{U}_i^k = \{y_i^s\}_{s=k}^3. \tag{10}$$

The successive decoding order at receiver y_i^k is summarized in Table I, and it proceeds as follows.

- **Receiver y_i^1:** In this state, the first baseline layer from the transmitter with the stronger channel is decoded. Since $\beta_1 < 1$, transmitter i has the stronger channel, and the layer V_i^1 is decoded first. In the next step, the baseline layer of the other transmitter V_j^1, where $j \neq i$, is decoded, followed by the remaining baseline layers $\{V_i^s\}_{s=2}^3$ from transmitter i. Finally, layer U_i^1 is decoded.
- **Receiver y_i^2:** In this state, the transmitters have the same channel gain $\beta_1 = 1$. In the first stage, the codebooks $\{V_i^1, V_j^1\}$, which are designated to be decodable by receiver y_i^1 are decoded. This is followed by decoding $\{V_i^2, V_j^2\}$, which are adapted to y_i^2. Then, the remaining baseline layer V_i^3 is decoded followed by codebooks $\{U_i^1, U_i^2\}$.
- **Receiver y_i^3:** In this state, the interfering link is stronger than the direct link, i.e., $\beta_3 > 1$. In this state, the procedure starts by decoding the baseline layer from the transmitter with the stronger channel, i.e., V_j^1, followed by the corresponding baseline layer from transmitter i, i.e., V_i^1. Then, layers $\{V_j^2, V_i^2\}$, which are decodable by receiver y_i^2 are decoded. Finally, layers $\{V_j^3, V_i^3\}$ that are adapted to receiver y_i^3 are decoded in addition to all the remaining layers $\{U_i^1, U_i^2, U_i^3\}$ from transmitter i.

D. Successive Decoding: ℓ-State Channel

Next, we generalize the successive decoding procedure in Table I. Similarly to (9) and (10) we define

$$\mathcal{V}_1^k = \{y_1^s\}_{s=1}^K \cup \{y_2^s\}_{s=k}^K, \tag{11}$$
$$\mathcal{V}_2^k = \{y_2^s\}_{s=1}^K \cup \{y_1^s\}_{s=k}^K, \tag{12}$$
$$\mathcal{U}_i^k = \{y_i^s\}_{s=k}^K. \tag{13}$$

Depending on the channel states, each of the two receivers decodes a subsets of the codebooks. Specifically, when the network state is (β_q, β_p), receiver 1 successively decodes $K+q$ and q codebooks from transmitters 1 and 2, respectively, over two stages. These codebooks are in particular adapted to receivers $\{y_1^s\}_{s=1}^q$.

- **Receiver 1 – stage 1** (Codebooks $\{V_i^s\}_{s=1}^q$): Receiver 1 decodes one layer from each user in an alternating manner until codebooks $\{V_1^s\}_{s=1}^q$ and $\{V_2^s\}_{s=1}^q$ are decoded. The first layer to be decoded in this stage depends on the state β_q. If $\beta_q < 1$, the receiver begins its decoding process by codebook V_1^1 from transmitter 1, then decodes the respective layer V_2^1 from transmitter 2, and continues alternating between the two transmitters. Otherwise, if $\beta_q > 1$, receiver 1 first decodes V_2^1 from the interfering transmitter 2, followed by V_1^1 from transmitter 1, and continues alternating. By the end of stage 1, receiver 1 has decoded q codebooks from each transmitter.
- **Receiver 1 – stage 2** (Codebooks $\{V_1^s\}_{s=q+1}^K$ & $\{U_1^s\}_{s=1}^q$): In stage 2, receiver 1 carries on decoding layers $\{V_1^s\}_{s=q+1}^K$ from transmitter 1, in an ascending order of the index s. Receiver 1 decodes layers $\{U_1^s\}_{s=1}^q$ specially adapted to receivers $\{y_1^s\}_{s=1}^q$, in an ascending order of index s. Throughout stage 2, receiver 1 has decoded K additional codebooks from transmitter 1.

Similarly, receiver 2 successively decodes $K+p$ codebooks from transmitter 2 and p codebooks from transmitter 1,

Authorized licensed use limited to: The Libraries at Rensselaer Polytechnic Institute. Downloaded on September 12,2022 at 21:48:32 UTC from IEEE Xplore. Restrictions apply.

TABLE II
SUCCESSIVE DECODING FOR $\ell-$ STATE CHANNEL

a_2 \ a_1	β_1	β_2	$\cdots$	β_q	$\cdots$	β_K
β_1	$\{V_1^s\}_{s=1}^K, U_1^1, V_2^1$ $\{V_2^s\}_{s=1}^K, U_2^1, V_1^1$	$\mathcal{C}_1^1, U_1^2, V_2^2$ $\mathcal{C}_2^1$	$\cdots$	$\cdot$	$\cdots$	$\mathcal{C}_1^{K-1}, U_1^K, V_2^K$ $\mathcal{C}_2^1$
β_2	$\mathcal{C}_1^1$ $\mathcal{C}_2^1, U_2^2, V_1^2$	$\mathcal{C}_1^1, U_1^2, V_2^2$ $\mathcal{C}_2^1, U_2^2, V_1^2$	$\cdots$	$\cdot$	$\cdots$	$\mathcal{C}_1^{K-1}, U_1^K, V_2^K$ $\mathcal{C}_2^1, U_2^2, V_1^2$
$\cdot$	$\cdot$	$\cdot$	$\cdots$	$\cdot$	$\cdots$	$\cdot$
β_p	$\cdot$	$\cdot$	$\cdots$	$\mathcal{C}_1^{q-1}, U_1^q, V_2^q$ $\mathcal{C}_2^{p-1}, U_2^p, V_1^p$	$\cdots$	$\cdot$
$\cdot$	$\cdot$	$\cdot$	$\cdots$	$\cdot$	$\cdots$	$\cdot$
β_K	$\mathcal{C}_1^1$ $\mathcal{C}_2^{K-1}, U_2^K, V_1^K$	$\mathcal{C}_1^1, U_1^2, V_2^2$ $\mathcal{C}_2^{K-1}, U_2^K, V_1^K$	$\cdots$	$\cdot$	$\cdots$	$\mathcal{C}_1^{K-1}, U_1^K, V_2^K$ $\mathcal{C}_2^{K-1}, U_2^K, V_1^K$

throughout two decoding stages that follow the same approach taken by receiver 1.

The set of decodable codebooks at receiver i in channel state (β_q, β_p) is related to set of codebooks decoded at receiver i and those decoded at receiver j in state $(\beta_{q-1}, \beta_{p-1})$. Table II specifies the set of the codebooks decoded in each network states. In this table, the channels are ordered in the ascending order. In particular, varying channels at receiver 1, state (β_q, β_p) precedes all channel states (β_k, β_p) for all $k > q$. Similarly, at receiver 2, state (β_q, β_p) precedes network state (β_q, β_k), for every $k > p$. Furthermore, according to this approach, when the *cross* channel of receiver i becomes stronger, receiver i decodes additional codebooks from both transmitters. In particular, in Table II, every cell contains the codebooks decoded in the combined channel state (β_q, β_p) where we mark the codebooks decoded by receiver 1 in black color, while those decoded by receiver 2 in red color. To further highlight the relationship between the decodable codebooks in different states, we denote by $\mathcal{C}_i^k$ the set of codebooks decoded by the receiver i when $a_i = \beta_k$.

E. Joint Decoding

Successive decoding compromises the achievable rate in favor of reducing decoding complexity. Specifically, in the second decoding scheme, we perform joint decoding, based on which we identify a tighter inner bound on the average capacity region. The decoding strategy at each of the decoders is listed in Table III. To formalize this, we define $\mathcal{S}_1^k$ (or $\mathcal{S}_2^k$) as the subset of interfering layers transmitted from transmitter 2 (or 1) and decoded by receiver y_1^k (or y_2^k). These sets, as specified in Table III, are given by

$$\mathcal{S}_1^k \triangleq \{V_2^s\}_{s=1}^k, \quad \text{and} \quad \mathcal{S}_2^k \triangleq \{V_1^s\}_{s=1}^k. \tag{14}$$

Similarly, we define $\mathcal{T}_1$ (or $\mathcal{T}_2$) as the subset of common intended layers transmitted from transmitter 1 (or 2) and decoded by its designated receiver. According to Table III, all common layers are decoded by the designated receiver in every channel state. Therefore, we have

$$\mathcal{T}_i \triangleq \{V_i^s\}_{s=1}^K. \tag{15}$$

The main difference between this joint decoding strategy and the strategy in Section III-D lies in the specific subset of codebooks $\{U_i^s\}_{s=1}^K$ decoded at receiver y_i^k. According to Table III, in joint decoding, codebook U_i^k is solely designated to and decoded by receiver y_i^k, whereas in the successive strategy in Section III-D, it is decoded by multiple receivers in $\mathcal{U}_i^k$. Such restrictions in the joint decoding strategy facilitate simplifying the inner bound on the achievable region presented in Section IV.

TABLE III
JOINT DECODING AT RECEIVERS $\{y_i^s\}_{s=1}^K$ IN $\ell-$ STATE CHANNEL

Receiver	Common layers	Private layers	Interfering layers
y_i^1	$\{V_i^s\}_{s=1}^K$	U_i^1	V_j^1
y_i^2	$\{V_i^s\}_{s=1}^K$	U_i^2	$\{V_j^s\}_{s=1}^2$
$\vdots$	$\vdots$	$\vdots$	$\vdots$
y_i^K	$\{V_i^s\}_{s=1}^K$	U_i^K	$\{V_j^s\}_{s=1}^K$

IV. AVERAGE RATE REGIONS

A. Average Achievable Rate Region

We characterize the interplay between the average rates of the two users. These rates are determined by the rates of the codebooks $\{V_i^k, U_i^k\}_{k=1}^K$, for $i \in \{1, 2\}$. The rates of the codebooks V_i^k and U_i^k are bounded by the minimum achievable rates at the receivers in the sets $\mathcal{V}_i^k$ and $\mathcal{U}_i^k$, respectively. We define $R(A)$ as the rate of the codebook $A \in \{V_i^k, U_i^k : \forall i, k\}$. Similarly, we define $\gamma(A)$ as the fraction of the power P_i allocated to the codebook $A \in \{V_i^k, U_i^k : \forall i, k\}$. Finally, we define $R_i(s, t)$ as the total achievable rate for user i in the network state (β_s, β_t), and define $\bar{R}_i \triangleq \mathbb{E}[R_i(\beta_s, \beta_t)]$ as the average achievable rate at receiver i, where the expectation is taken with respect to the probabilistic model of the channel states. By noting that overall the transmitters have $4K$ codebooks, corresponding to $\mathcal{S}$ as a subset of the $4K$-dimensional space $\mathbb{R}_+^{4K}$, we define the rate region $\mathcal{R}_{\text{in}}(\mathcal{S})$ as the set of all average rate combinations $(\bar{R}_1, \bar{R}_2)$ such that $R(A) \in \mathcal{S}$ for all $A \in \{V_i^k, U_i^k : \forall i, k\}$, i.e.,

$$\mathcal{R}_{\text{in}}(\mathcal{S}) \triangleq \left\{(\bar{R}_1, \bar{R}_2) \ : \ R(A) \in \mathcal{S}, \ \forall A \in \{V_i^k, U_i^k : \forall i, k\}\right. . \tag{16}$$

To characterize the achievable rate region of the proposed approach, corresponding to each receiver y_i^k and codebook $A \in \{U_i^k, V_i^k : \forall i, k\}$ that should be decoded by y_i^k,

Authorized licensed use limited to: The Libraries at Rensselaer Polytechnic Institute. Downloaded on September 12,2022 at 21:48:32 UTC from IEEE Xplore. Restrictions apply.

we define $R_i^k(A)$ as the maximum rate that we can sustain for codebook A, while being decodable by y_i^k when using the proposed encoding and decoding schemes. Accordingly, for user i, and corresponding to $s,t \in \{1,\ldots,K\}$ we define

$$r_i(s,t) \triangleq \sum_{k=t+1}^{K} R_i^s(V_i^t) + \sum_{k=1}^{s} R_i^k(U_i^k) \tag{17}$$

$$+ \min_{j_k \in \{1,2\}} \sum_{k=1}^{t} R_{j_k}^k(V_i^k). \tag{18}$$

Theorem 1 (Inner Bound via Sequential Decoding): The average achievable rate region via sequential decoding is specified by

$$\mathcal{R}_{\text{in}}^{\text{seq}} \triangleq \left\{(\bar{R}_1,\bar{R}_2) \ : \ R_i(s,t) \le r_i(s,t),\ \forall i,s,t\right\}. \tag{19}$$

Proof: See Appendix I. ∎

Next, we provide an average achievable rate region for the 2-user channel in which the receivers deploy joint decoding. For this purpose, we define the following rate region in $\mathbb{R}_+^{12}$ that captures the interplay between the rates of all 12 codebooks $\{V_i^k, U_i^k : \forall i,k\}$ in the two-state channel.

$$\mathcal{R}_{\text{in}}^{12} \triangleq \Bigg\{ R(\mathcal{U},\mathcal{V}) \ : \ \text{that satisfies } \forall \mathcal{A}\subseteq\mathcal{T}_1,\ \mathcal{B}\subseteq\mathcal{S}_1^k : \sum_{j:V_1^j\in\mathcal{A}} R(V_1^j) + R(U_1^k) + \sum_{j:V_2^j\in\mathcal{B}} R(V_2^j) \le r_1^k(\mathcal{A},\mathcal{B}),$$

$$\text{and } \forall \mathcal{A}\subseteq\mathcal{T}_2,\ \mathcal{B}\subseteq\mathcal{S}_2^k : \tag{20}$$

$$\sum_{j:V_2^j\in\mathcal{A}} R(V_2^j) + R(U_2^k) + \sum_{j:V_1^j\in\mathcal{B}} R(V_1^j) \le r_2^k(\mathcal{A},\mathcal{B}) \Bigg\} \tag{21}$$

where we have defined

$$R(\mathcal{U},\mathcal{V}) \triangleq (R(U_1^1),\ldots,R(V_2^1),\ldots,R(V_2^3)), \tag{22}$$

and for $\mathcal{A}\subseteq\mathcal{T}_1$ and $\mathcal{B}\subseteq\mathcal{S}_1^s$ we have defined $r_1^s(\mathcal{A},\mathcal{B})$ in (23), as shown at the bottom of the next page. and for $\mathcal{A}\subseteq\mathcal{T}_2$ and $\mathcal{B}\subseteq\mathcal{S}_2^s$, we have defined $r_2^s(\mathcal{A},\mathcal{B})$ in (24), as shown at the bottom of the next page.

Theorem 2 (Inner Bound via Joint Decoding): In the two-state channel, the average achievable rate region via joint decoding encloses the is specified by

$$\mathcal{R}_{\text{in}}^{\text{joint}} \triangleq \left\{(\bar{R}_1,\bar{R}_2) : R(A)\in\mathcal{R}_{\text{in}}^{12},\quad \forall A\in\{V_i^k,U_i^k : \forall i,k\}\right\}. \tag{25}$$

Proof: See Appendix II. ∎

B. Sum-Rate Gap Analysis

Next, we leverage the encoding and decoding schemes in section III to characterize the gap to the average capacity. For the successive decoding scheme in Section III-D, we focus on characterizing the gap to the sum-rate capacity when transmitters have full CSIT in all SNR regimes.

1) Successive Decoding & Sum-Rate Capacity: In this subsection, we characterize the gap between the sum-rate achievable by the proposed adaptive layering and successive decoding schemes, and the sum-rate capacity when the transmitters have full CSIT. Furthermore, we demonstrate that in the high SNR regime, the gap is upper bounded by a constant. In order to place the emphasis on the main ideas, we focus on the symmetric setting, i.e., $a_1 = a_2 = a$, symmetric average power constraints, i.e., $P_1 = P_2 = P$, and symmetric probabilistic models for the channels, i.e., $q_1^s = q_2^s = q^s = \frac{1}{3}$. The results can be readily generalized to the non-symmetric setting at the expense of a higher parameterization dimension.

In the symmetric case, the interference channel specified by (6) reduces to either a weak interference channel (when $a = \beta_1$), or to a strong interference channel (when $a \in \{\beta_2,\beta_3\}$). To quantify the average sum-rate gap, we start by analyzing the gap in the weak and strong interference regimes separately, the average of which subsequently provides the average sum-rate gap. Throughout this subsection we set $\beta \triangleq \beta_3 = \frac{1}{\beta_1}$.

- **Weak interference:** In this setting, the capacity with full CSIT is, in general, unknown. Hence, we quantify the gap between our average sum-rate and that of HK with full-CSIT. Subsequently, by leveraging the known results on the gap between HK's sum-rate and the sum-rate capacity, we delineate an upper bound on the average sum-rate gap of interest. In particular, we consider the simple scheme of [5] in which the effective power of some messages is normalized to 1 at each receiver. This simple HK scheme is known to achieve a sum-rate within 2-bits from the sum-rate capacity. Note that in the case of weak interference, the achievable sum-rate of the HK-scheme in [5], depending on the channel parameters, is either bounded by the capacity of the multiple access channel formed at each receiver, or by the constraint on the rate of the common message at the *unintended* receiver. These two different regimes are identified by the relationship between the power constraint P, and the channel gains $\{\frac{1}{\beta},1,\beta\}$.
- **Strong interference:** For the case of a strong interference channel, the sum-rate capacity with full CSIT is known. It can be characterized by evaluating the sum-rate of the intersection of two capacity regions corresponding to two multiple access channels formed by the transmitters and each of the receivers [7].

Subsequently, upper bounds on the gap between the average sum-rate achieved by the approach in Section III and the sum-rate capacity is established in the following theorem. The gap is characterized in two transmission power regimes, denoted by G_1 and G_2. We define $\bar{R}_{\text{sum}}(\text{G}_i)$ as the minimum average sum-rate achievable under region G_i, and denote the average sum-rate capacity with full CSIT by $C_{\text{sum}}(\text{G}_i)$. Finally, we define the gap $\Delta(G_i) \triangleq C_{\text{sum}}(\text{G}_i) - \bar{R}_{\text{sum}}(\text{G}_i)$.

Theorem 3: The average sum-rate achievable by the broadcast approach in Fig. 2 and Table I has the following gap with the sum-rate capacity of the symmetric Gaussian interference channel with full CSIT:

Authorized licensed use limited to: The Libraries at Rensselaer Polytechnic Institute. Downloaded on September 12,2022 at 21:48:32 UTC from IEEE Xplore. Restrictions apply.

(i) For $P \in \mathrm{G}_1 \triangleq (0,\beta) \cup \left(\beta(\beta^2+\beta-1), +\infty\right)$ we have

$$\Delta(\mathrm{G}_1) \leq \frac{1}{3}\left[1 + \log\left(\frac{1+P(1+\beta)}{1+P(1+\frac{1}{\beta})}\right) + \frac{1}{2}\log(2+\beta)\right]. \tag{26}$$

(ii) For $P \in \mathrm{G}_2 \triangleq \left[\beta, \beta(\beta^2+\beta-1)\right]$ we have

$$\Delta(\mathrm{G}_2) \leq \frac{1}{3}\left[\log\frac{4}{3} + \log\left(\frac{1+P(1+\beta)}{1+P/\beta+\beta}\right) + 3\log\frac{(2+\beta)^2}{1+2\beta}\right]. \tag{27}$$

Proof: See Appendix III. ∎

Next, we show that the gap in the high SNR regime is upper bounded by a constant.

Theorem 4: For any fixed network model (i.e., fixed β), when P is sufficiently large, the gap between the sum-rate capacity of the symmetric Gaussian interference channel with full CSIT and the average sum-rate achievable by the proposed broadcast approach in Fig. 2 and Table I is upper bounded by

$$\Delta \leq \tfrac{1}{6}\log\left(8\beta^2 \cdot \tfrac{\beta+2}{\beta+1}\right). \tag{28}$$

Proof: It follows from finding the limit of $\lim_{P\to\infty}\Delta(\mathrm{G}_1)$ in (28). ∎

V. Generalization to the N-User Channel

Consider a generalization of (2) to the N-user channel, in which for user m we have

$$y_m = x_m \; + \; \textstyle\sum_{i\neq m}\sqrt{a_{mi}}x_i \; + \; n_m. \tag{29}$$

Each of the channel coefficients a_{im} takes one of the L possible states $\{\beta_1,\ldots,\beta_L\}$, order in the ascending order. The state of the network will be specified by the cross-links states, rendering a network with N transmitters and NL^{N-1} receivers. In the case of the symmetric interference channel, i.e., $a_{mi} = a$, the number of network states reduces to N transmitters and NL receivers.

To balance its impacts on the intended and unintended receivers, each transmitter adopts rate-splitting and adapts each information layer to one combined state of the network designated to be decoded by a specific group of receivers. In the equivalent network, each transmitter and its associated $S \triangleq L^{N-1}$ receivers form a multiple access channel. The critical stage in specifying the broadcast approach is designing a notion of degradedness among different such multiple access channels. Facing a lack of a natural choice, we define an aggregate strength for receiver y^m as

$$\theta_m \triangleq \sum_{i\neq m} a_{mi}. \tag{30}$$

We use this metric to sort the S receivers associated with y^m in the equivalent network. We denote these receivers by $\{y_m^1,\ldots,y_m^S\}$, which are sorted in the ascending order such that for $s<k$ receivers, the θ_m value associated with the states in the channel receiver y_i^s is smaller than that of receiver y_i^k. Hence, for $s<k$, the multiple access channel at receiver y_i^s is degraded with respect to the channel at y_i^k. Therefore, receiver y_i^k can successfully decode all the layers adapted to the channels with the designated receivers $\{y_i^1,\ldots,y_i^s\}$. At receiver y_i^k, every layer decoded form transmitter i directly increases the achievable rate, whereas every layer decoded from the other transmitter indirectly increases the achievable rate by canceling a part of the interfering signal. Hence, similarly to the two-user channel, transmitter i splits its message into $2S$ layers denoted by $\{V_i^k, U_i^k\}_{k=1}^S$ with the following designations and objectives:

- Transmitter m adapts layer V_m^k to the state of the channels linking all other transmitters to the *unintended* receivers $\{y_1^k,\ldots,y_{N^{L-1}}^k\}\backslash\{y_m^k\}$: while the intended receivers $\{y_m^k\}_{k=1}^S$ will be decoding all codebooks $\{V_m^k\}_{k=1}^S$, the non-intended receivers $\{y_1^k,\ldots,y_S^k\}\backslash\{y_m^k\}$ decode a subset of these codebooks depending on their channel strengths. More specifically, a non-intended receiver y_i^k decodes only the codebooks $\{V_m^s\}_{s=1}^k$.
- Transmitter m adapts the layer U_m^k to the state of the channels linking all other transmitters to the *intended* receiver y_m^k: while the unintended receivers $\{y_1^k,\ldots,y_S^k\}\backslash\{y_m^k\}$ will *not* be decoding any of the codebooks $\{U_m^k\}_{k=1}^S$, the intended receivers $\{y_m^k\}_{k=1}^S$ decode a subset of these codebooks depending on their channel strengths. More specifically, the intended receiver y_m^k decodes only the codebooks $\{U_m^s\}_{s=1}^k$.

As the number of users N increases, the total number of codebooks per transmitter $2S = 2L^{N-1}$ grows exponentially with the number of users. This renders joint decoding to have a prohibitive decoding complexity. We can adopt the opportunistic successive decoding schemes in [19], [57], which are low-complexity schemes in which each receiver can dynamically identify an optimal set of codebooks to decode.

VI. Numerical Evaluations

In this section, we provide numerical evaluations, with the main objective of comparing the proposed approach's performance without CSIT with that of the HK approach with the CSIT. In figures 3 and 4, we compare the maximum average sum-rate in our approach with that of the HK. In both schemes, the average sum-rate is maximized over all possible power allocation schemes over different codebooks. Figure 3

$$r_1^s(\mathcal{A},\mathcal{B}) \triangleq C\left(\gamma(U_1^s)P_1 + \sum_{k:V_1^k\in\mathcal{A}}\gamma\left(V_1^k\right)P_1 + \beta_s\sum_{t:V_2^t\in\mathcal{B}}\gamma\left(V_2^t\right)P_2, \sum_{k\neq s}\gamma\left(U_1^k\right)P_1 + \beta_1\sum_{t:V_2^t\in\mathcal{B}^c}\gamma\left(V_2^t\right)P_2\right). \tag{23}$$

$$r_2^s(\mathcal{A},\mathcal{B}) \triangleq C\left(\gamma(U_2^s)P_2 + \sum_{k:V_2^k\in\mathcal{A}}\gamma\left(V_2^k\right)P_2 + \beta_s\sum_{t:V_1^t\in\mathcal{B}}\gamma\left(V_1^t\right)P_1, \sum_{k\neq s}\gamma\left(U_2^k\right)P_1 + \beta_1\sum_{t:V_1^t\in\mathcal{B}^c}\gamma\left(V_1^t\right)P_1\right). \tag{24}$$

Authorized licensed use limited to: The Libraries at Rensselaer Polytechnic Institute. Downloaded on September 12,2022 at 21:48:32 UTC from IEEE Xplore. Restrictions apply.

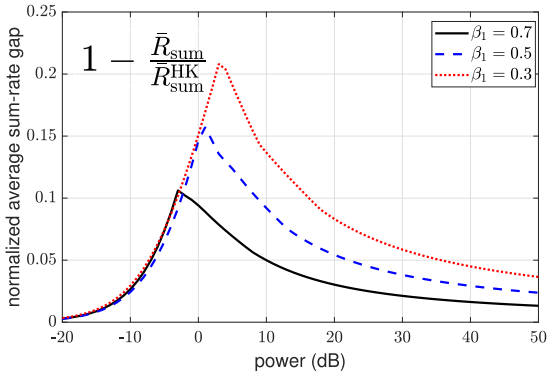

Fig. 3. Sum-rate gap versus power.

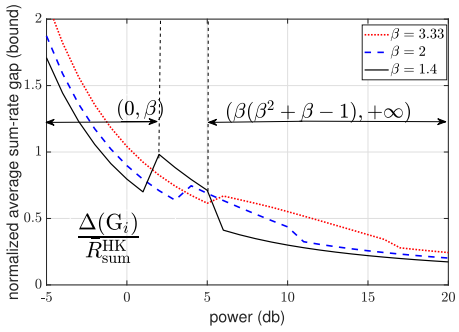

Fig. 4. Bound on sum-rate gap versus power.

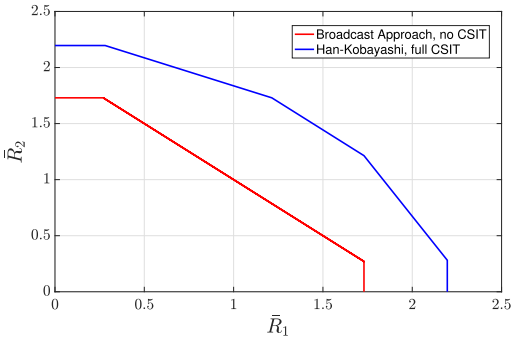

Fig. 5. Average rate region ($\ell=2$).

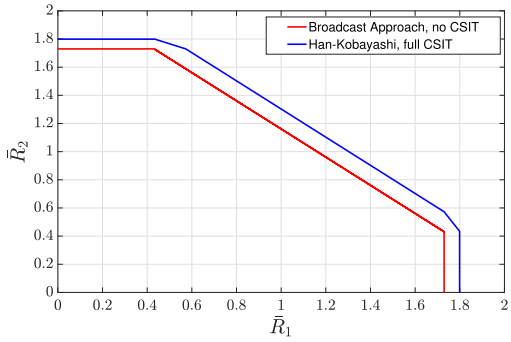

Fig. 6. Average rate region ($\ell=3$).

depicts the gap between the two methods normalized by the sum-rate of HK. This signifies the relative sum-rate loss that can be attributed, for the most part, to the lack of the CSI at the transmitters. It is observed that the relative loss with respect to the HK peaks for moderate power regimes, while in the small and large power regimes, it is diminishing. For the evaluations in Fig. 3, we consider a two-state channel, with a symmetric channel probability model ($q_1^s=q_1^s=q^s$), in which we have set $(q^1,q^2,q^3)=(0.3,0.6,0.1)$. The results follow the same trend for different values of β_1. Figure 4 evaluates the bounds on the sum-rate gaps presented in Theorem 3. The three plots in this figure correspond to those in Fig. 3. Specifically, the plots in Fig. 4 depict the $\Delta(\ \mathrm{G}_i)$ normalized by the HK sum-rate. This figure shows that the bounds on the gap become tighter as the power increases.

A multi-layer superposition coding with joint decoding for the compound Gaussian interference channel in [47] is shown to achieve an achievable rate region as close as 1 bit within an outer bound on the capacity region of that channel. Even though it is shown in [13] that successive decoding with time-sharing fails to replace the simultaneous joint decoding in the presence of two receivers in the interference channel, as the number of channel states, and accordingly the number of information layers required, increase, the optimal power allocation for joint decoding becomes computationally demanding. Figure 3 shows that by limiting the interference in each channel state at each receiver to 1, successive decoding offers comparable performance compared to the joint decoding without CSIT and even HK schemes with full CSIT. We remark that to limit the interfering signal from the unintended receivers, directly identify the power allocation of the common messages of each transmitter and the power allocation of the baseline private layer as a function of the channel parameters.

We evaluate the average achievable rate region characterized in Theorem 1. Figure 5 demonstrates a general asymmetric setting for the following set of parameters $P_1=P_2=10$ dB, $(q_1^1,q_1^2,q_1^3)=(0.5,0.3,0.2)$, $(q_2^1,q_2^2,q_2^3)=(0.3,0.3,0.4)$, and the weak channel state at each receiver is given by $\beta_1=0.5$. Similarly, for $\ell=3$ we evaluate the average rate region characterized in Theorem 1 in Figure 6 for the general asymmetric channel with $(q_i^1,q_i^2,q_i^3,q_i^4,q_i^5,q_i^6,q_i^7)=(0.1,0.1,0.1,0.2,0.1,0.1,0.3)$, and the weak channel states at each receivers 1 and 2 are set as $(\beta_1,\beta_2,\beta_3)=(0.1,0.2,0.9)$ and $(\beta_1,\beta_2,\beta_3)=(0.1,0.4,0.7)$, respectively. Comparing these figures suggest that increasing the number of states leads to a shrinking gap between the two regions (broadcast approach and HK) as the number of states increases. This is due to the fact that as the number of the states increases, the transmitter has a better chance of distributing its resources to codebooks adapted to different channels.

In Figure 7, we compare the variations of normalized average sum-rates versus β_1 in three different settings: HK, rate-splitting and the successive decoding scheme in Section III-C, and rate-splitting and the joint decoding scheme in Section III-E. We consider a general setting with asymmetric channel parameters. We set $P_1=P_2=10$ dB, $(q_1^1,q_1^2,q_1^3)=(0.1,0.5,0.4)$, $(q_2^1,q_2^2,q_2^3)=(0.7,0.1,0.2)$, and the weak channel state at receiver 1 is set $\beta_1=0.2$. This figure shows partly the cost of the lack of CSIT. It also shows,

Authorized licensed use limited to: The Libraries at Rensselaer Polytechnic Institute. Downloaded on September 12,2022 at 21:48:32 UTC from IEEE Xplore. Restrictions apply.

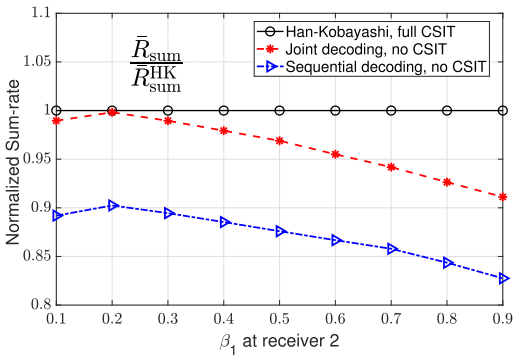

Fig. 7. Sum-rate versus β_1.

as expected, joint decoding performs (slightly) better at the expense of (sometimes significant) more decoding complexity.

VII. Conclusion

In this article, we have proposed a novel distributed interference management scheme based on the broadcast approach. First, we have considered the two-user finite-state Gaussian interference channel in which each transmitter is oblivious to all channel states. Based on the combined network state, a multi-layer superposition coding scheme is adopted at each transmitter combined with an opportunistic decoding scheme at the receivers. We have proposed a simple successive decoding order, for which we have characterized the average achievable rate region. Furthermore, we have shown that in the high signal-to-noise ratio regime, the corresponding sum-rate lies within a finite gap of the sum-rate capacity of the interference channel with full channel state information. We have also characterized an average achievable rate region using joint decoding, as well as an upper bound on the average capacity region. Finally, we have presented the generalization of the proposed approach to the case of an arbitrary number of users. Some important open directions to investigate include various interference channel models with more users, the intimate connection between the proposed transmission scheme and distributed source coding over interference channels with successive refinement [69], and application of the broadcast approach and distributed caching over interference channels to determine caching what layers can best enhance interference management [70].

Appendix I
Proof of Theorem 1

We define $\gamma(A)$ as the fraction of P_i allocated to $A \in \{U_i^k, V_i^k : \forall k\}$, and define

$$\Gamma_v(i,k) \triangleq \sum_{j=1}^{k} \gamma(V_i^j), \quad \text{and } \Gamma_u(i,k) \triangleq \sum_{j=1}^{k} \gamma(U_i^j). \tag{31}$$

Based on these definitions, if the codebook V_i^k is decoded by the receiver y_i^s, then we have

$$\begin{aligned}\text{If } \beta_s \le 1: \quad R_i^s(V_i^k) = C(&\gamma(V_i^k)P_i, (1-\Gamma_v(i,k))P_i \\ &+ \beta_k(1-\Gamma_v(j,s-1))P_j),\end{aligned} \tag{32}$$

$$\begin{aligned}\text{If } \beta_s > 1: \quad R_i^s(V_i^k) = C(&\gamma(V_i^k)P_i, (1-\Gamma_v(i,k))P_i \\ &+ \beta_k(1-\Gamma_v(j,s))P_j).\end{aligned} \tag{33}$$

Similarly, if the codebook V_i^k is decoded by the receiver y_j^s, then we have

$$\begin{aligned}\text{If } \beta_s \le 1: \quad R_j^s(V_i^k) = C(&\beta_s\gamma(V_i^k)P_i, \beta_k(1-\Gamma_v(i,k))P_i \\ &+ (1-\Gamma_v(j,s))P_j),\end{aligned} \tag{34}$$

$$\begin{aligned}\text{If } \beta_s > 1: \quad R_j^s(V_i^k) = C(&\beta_s\gamma(V_i^k)P_i, \beta_k(1-\Gamma_v(i,k))P_i \\ &+ (1-\Gamma_v(j,s-1))P_j).\end{aligned} \tag{35}$$

Finally, when codebook U_i^k is decoded by the receiver y_i^s, then we have

$$\begin{aligned}R_i^s(U_i^k) = C(&\gamma(U_i^k)P_i, \beta_k(1-\Gamma_v(1,s))P_j \\ &+ (1-\Gamma_v(1,K)-\Gamma_u(1,s))P_i).\end{aligned} \tag{36}$$

In the rates specified above, P_i is the power of transmitter i, and P_j is the power of the other transmitter. We provide the proof for $\ell = 2$. The general setting follows the same steps. The rates of codebooks V_i^k and U_i^k, for each i, k, are bounded by the smallest rate that ensures they are decodable by all the receivers in the sets $\mathcal{V}_i^k$ and $\mathcal{U}_i^k$ defined in (9) and (10), respectively. According to the broadcast channel model in (6), the state of each receiver is determined by the *cross* channel gain $a_i \in \{\beta_1, \beta_2, \beta_3\}$. The maximum achievable rates at each receiver are determined by the direct and cross channel gains at that receiver only. The successive decoding order in Table I enforces a set of upper bounds on the rates for each receiver y_i^k.

Receiver y_1^1: At receiver y_1^1, codebooks $\{V_1^1, V_1^2, V_1^3, U_1^3\}$ are decoded from transmitter 1 in addition to codebook V_2^1 from transmitter 2. This results in the following set of rate bounds.

$$R(A) \le R_1^1(A) \quad \text{for} \quad A \in \{V_1^1, V_1^2, V_2^1, V_1^3, U_1^1\}. \tag{37}$$

Receiver y_1^2: At receiver y_1^2, in addition to decoding the set of layers previously decoded by receiver y_1^1, the stronger *cross* channel decodes an additional interfering layer, i.e., V_2^2. Opportunistically, it can also decode an additional layer from transmitter 1, i.e., U_1^2. This decoding scheme indicates the following constraints.

$$R(A) \le R_1^2(A) \quad \text{for } A \in \{V_1^1, V_2^1, V_1^2, V_2^2, V_1^3, U_1^1, U_1^2\}. \tag{38}$$

Receiver y_1^3: Finally, at receiver y_1^3, a stronger *cross* channel state allows an additional layer from the interfering signal, V_2^3, to be decoded. All the encoded layers received from transmitter 1 can also be decoded.

$$R(A) \le R_1^3(A) \text{ for } A \in \{V_1^1, V_2^1, V_1^2, V_2^2, V_1^3, V_2^3, U_1^1, U_1^2, U_1^3\}. \tag{39}$$

Similarly, we find the counterpart rate constraints for receivers y_2^1, y_2^2, and y_2^3. Next, we leverage the conditions specified in (37)-(38) to characterize the average achievable rate region in Theorem 1. We start by characterizing the aggregate achievable rate region for both transmitters in each channel state by

Authorized licensed use limited to: The Libraries at Rensselaer Polytechnic Institute. Downloaded on September 12,2022 at 21:48:32 UTC from IEEE Xplore. Restrictions apply.

using Fourier-Motkinz elimination (FME). To this end, note that even though the set of codebooks decoded at receiver i depends only on the state of a_i, the total achievable rate $R_i(s,t)$ is influenced by the rate bounds enforced by both receivers through partly decoding the common codebooks. For channel state (β_1,β_1), we directly follow the FME procedure to sequentially eliminate the layered codebooks. First, in (37) and (38), we replace $R(U_1^1)$ by $(R_1(1,1)-\sum_{k=1}^{3}R(V_1^k))$, and replace $R(U_2^1)$ by $(R_2(1,1)-\sum_{k=1}^{3}R(V_2^k))$. Subsequently, we sequentially eliminate the remaining variables, i.e., $\{R(V_1^k)\}_{k=1}^3,\{R(V_2^k)\}_{k=1}^3$. For all $k\in\{1,2,3\}$, we collect all inequalities that have the term $R(V_1^k)$ with a negative sign resulting in

$$R_1(1,1)-\sum_{k=1}^{3}R(V_1^k)\leq R_1^1(U_1^1). \tag{40}$$

Finally, we add (40) to all inequalities in (37) and (38) (all those that contain $R(V_1^k)$) resulting in

$$R_1(1,1)\leq\sum_{k=2}^{3}R_1^1(V_1^k)+R_1^1(U_1^1)+\min_{j\in\{1,2\}}R_j^1(V_1^1)\triangleq r_1(1,1). \tag{41}$$

By sequentially eliminating the layers decoded by receiver 2, arriving at

$$R_2(1,1)\leq\sum_{k=2}^{3}R_2^1(V_2^k)+R_2^1(U_2^1)+\min_{j\in\{1,2\}}R_j^1(V_2^1)\triangleq r_2(1,1). \tag{42}$$

Moving on to channel state (β_1,β_2), we directly apply the FME process using (37) and its counterparts for receiver 2, arriving at the following average achievable rates

$$\begin{aligned}R_1(1,2)&\leq R_1^1(V_1^3)+R_1^1(U_1^1)+\min_{\ell,n\in\{1,2\}}R_1^1(V_1^\ell)+R_2^2(V_1^n)\\&\triangleq r_1(1,2),\\R_2(1,2)&\leq\sum_{k=2}^{3}R_2^2(V_2^k)+\sum_{k=1}^{2}R_2^2(U_2^k) \qquad (43)\\&\quad+\min\{R_1^1(V_2^1),R_2^2(V_2^1)\}\triangleq r_2(1,2). \qquad (44)\end{aligned}$$

Similarly, the average achievable rates in state (β_1,β_3) are bounded by

$$\begin{aligned}R_1(1,3)&\leq\sum_{k=1}^{3}R_1^1(V_1^k)+R_1^1(U_1^1)\triangleq r_1(1,3)\,, \qquad (45)\\R_2(1,3)&\leq\sum_{k=2}^{3}R_2^3(V_2^k)+\sum_{k=1}^{3}R_2^3(U_2^k)\\&\quad+\min\{R_1^1(V_2^1),R_2^3(V_2^1)\}\triangleq r_2(1,3)\,. \qquad (46)\end{aligned}$$

For the remaining network states, we have the following average achievable rates bounds

$$\begin{aligned}R_1(2,1)&\leq\sum_{k=2}^{3}R_1^2(V_1^k)+\sum_{k=1}^{2}R_1^2(U_1^k)\\&\quad+\min\{R_2^1(V_1^1),R_1^2(V_1^1)\}\triangleq r_1(2,1), \qquad (47)\\R_2(2,1)&\leq R_2^1(V_2^3)+R_2^1(U_2^1)\\&\quad+\min_{\ell,n\in\{1,2\}}R_2^1(V_2^\ell)+R_1^2(V_2^n)\triangleq r_2(2,1)\,, \qquad (48)\\R_1(2,2)&\leq\sum_{k=1}^{3}R_1^2(V_1^k)+\sum_{k=1}^{2}R_1^2(U_1^k)\triangleq r_1(2,2)\,, \qquad (49)\\R_2(2,2)&\leq\sum_{k=1}^{3}R_1^2(V_2^k)+\sum_{k=1}^{2}R_2^2(U_2^k)\triangleq r_2(2,2)\,, \qquad (50)\\R_1(2,3)&\leq\sum_{k=1}^{3}R_1^2(V_1^k)+\sum_{k=1}^{3}R_1^2(U_1^k)\triangleq r_1(2,3)\,, \qquad (51)\\R_2(2,3)&\leq\sum_{k=1}^{3}R_2^3(V_2^k)+\sum_{k=1}^{3}R_2^3(U_2^k)\triangleq r_2(2,3). \qquad (52)\end{aligned}$$

The last set of average rate bounds correspond to network states $(\beta_3,\beta_k),\forall k\in\{1,2,3\}$ stated as follows.

$$\begin{aligned}R_1(3,1)&\leq\sum_{k=2}^{3}R_1^3(V_1^k)+\textstyle\sum_{k=1}^{3}R_1^3(U_1^k)\\&\quad+\min\{R_2^1(V_1^1),R_1^3(V_1^1)\}\triangleq r_1(3,1), \qquad (53)\\R_2(3,1)&\leq\sum_{k=1}^{3}R_2^1(V_2^k)+R_2^1(U_2^1)\triangleq r_2(3,1), \qquad (54)\\R_1(3,2)&\leq\sum_{k=1}^{3}R_1^3(V_1^k)+\sum_{k=1}^{3}R_1^3(U_1^k)\triangleq r_1(3,2)\,, \qquad (55)\\R_2(3,2)&\leq\sum_{k=1}^{3}R_2^2(V_2^k)+\sum_{k=1}^{3}R_2^2(U_2^k)\triangleq r_2(3,2)\,, \qquad (56)\\R_1(3,3)&\leq\sum_{k=1}^{3}R_1^3(U_1^k)\\&\quad+\min_{n,\ell,p\in\{1,2\}}R_n^3(V_1^1)+R_\ell^3(V_1^2)+R_p^3(V_1^3)\\&\triangleq r_1(3,3)\,, \qquad (57)\\R_2(3,3)&\leq\sum_{k=1}^{3}R_2^3(U_2^k)\\&\quad+\min_{n,\ell,p\in\{1,2\}}R_n^3(V_2^1)+R_\ell^3(V_2^2)+R_p^3(V_2^3)\\&\triangleq r_2(3,3). \qquad (58)\end{aligned}$$

Finally, using (41)-(58), the average achievable rate regions are specified by those given in (19).

We start by describing the procedure of the codebook generation at each user. Subsequently, we identify the encoding and decoding policies at each receiver, followed by error probability analysis.

Authorized licensed use limited to: The Libraries at Rensselaer Polytechnic Institute. Downloaded on September 12,2022 at 21:48:32 UTC from IEEE Xplore. Restrictions apply.

APPENDIX II
PROOF OF THEOREM 2

Encoding: The codebook generation scheme dictates adapting the layers of each transmitter to different channel states. The achievable scheme is designated by the set of an ordered random variables

$$\{Q, V_i^1, V_i^2, V_i^3, U_i^1, U_i^2, U_i^3\}, \tag{59}$$

with joint distribution $\mathcal{P}_i$ corresponding to transmitter i. The achievable scheme consists of multi-level superposition coding. It starts with an ordered generation of codewords associated with the ordered random variables in (59). Specifically, we generate a codeword $Q^{(n)}$ of length n that consists of n independent and identically distributed (i.i.d.) random variables according to $\prod_{t=1}^{n} p(q_t)$. For codeword $Q^{(n)}$, we then generate $2^{nR(V_1^1)}$ independent codewords

$$V_1^{1(n)}(j_1), \quad j_1 \in \left\{1, \ldots, 2^{nR(V_1^1)}\right\}, \tag{60}$$

$$V_1^{2(n)}(k_1), \quad k_1 \in \left\{1, \ldots, 2^{nR(V_1^2)}\right\}, \tag{61}$$

$$V_1^{3(n)}(\ell_1), \quad \ell_1 \in \left\{1, \ldots, 2^{nR(V_1^3)}\right\}. \tag{62}$$

such that each element of codeword $V_1^{k(n)}$ is i.i.d. according to $\prod_{t=1}^{n} p(v_1^{st}|q_t)$. For each set of codewords $\{V_1^{1(n)}(j_1), V_1^{2(n)}(k_1), V_1^{3(n)}(\ell_1)\}$, it generates $2^{nR(U_1^1)}$ i.i.d. codewords

$$U_1^{1(n)}(j_1, k_1, \ell_1, m_1), \quad m_1 \in \left\{1, \ldots, 2^{nR(U_1^1)}\right\}, \tag{63}$$

according to $\prod_{t=1}^{n} p(u_{1t}^1|v_{1t}^3, v_{1t}^2, v_{1t}^1, q_t)$. Similarly, it generates $2^{nR(U_1^2)}$ i.i.d. codewords

$$U_1^{2(n)}(j_1, k_1, \ell_1, n_1), \quad n_1 \in \left\{1, \ldots, 2^{nR(U_1^2)}\right\}, \tag{64}$$

according to $\prod_{t=1}^{n} p(u_{1t}^2|v_{1t}^1, v_{1t}^2, v_{1t}^3, q_t)$. Finally, it generates $2^{nR(U_1^3)}$ independent codewords

$$U_1^{3(n)}(j_1, k_1, \ell_1, x_1), \quad x_1 \in \left\{1, \ldots, 2^{nR(U_1^3)}\right\}, \tag{65}$$

such that each element is i.i.d. according to $\prod_{t=1}^{n} p(u_{1t}^3|v_{1t}^1, v_{1t}^2, v_{1t}^3, q_t)$. User 2 generates in a similar fashion. Accordingly, transmitter i communicates the message indexed by $(j_i, k_i, \ell_i, m_i, n_i, x_i)$ by sending the superposition of the codewords in the set defined in (66), as shown at the bottom of the next page.

Decoding Scheme: We focus on outlining the decoding scheme of receiver 1 and the decoding scheme at receiver 2 follows similarly. Receivers $\{y_1^k : k \in \{1,2,3\}\}$ perform jointly typical set decoding. We denote the set of the jointly typical sequences χ^n by $A_\epsilon^{(n)}(\Lambda)$, where Λ denotes the probability space of the collection of random variables. In network state (β_1, β_j), receiver y_1^1 determines a unique tuple $(\hat{j}_1, \hat{k}_1, \hat{\ell}_1, \hat{m}_1)$ and any $\hat{j}_2$ such that the event in (67), as shown at the bottom of the next page. An error is declared if receiver y_1^1 fails to find such a sequence. In channel state (β_2, β_j), receiver y_1^2 determines a unique $(\hat{j}_1, \hat{k}_1, \hat{\ell}_1, \hat{n}_1)$ and any $(\hat{j}_2, \hat{k}_2)$ such that the event in (68), as shown at the bottom of the next page. An error is declared if receiver y_1^2 fails to find such sequence. Finally, in channel state (β_3, β_j), receiver y_1^3 determines a unique $(\hat{j}_1, \hat{k}_1, \hat{\ell}_1, \hat{x}_1)$ and any $(\hat{j}_2, \hat{k}_2, \hat{\ell}_2)$ such that the event in (69), as shown at the bottom of the next page. An error is declared if receiver y_1^3 fails to find such a sequence.

Error Probability Analysis: We start our analysis by considering the network state (β_1, β_j), which results in the set of bound given in (72)-(91). Note that based on the assumptions that the messages are picked uniformly at random and that the probability of error is averaged over the ensemble of the generated codebooks, the probability of error does not depend on a specific choice codeword. Therefore, without loss of generality, we assume that the message transmitted by transmitters are $(1,1,1,1,1,1)$. We define the following event $E_{i_1\ j_1\ k_1\ell_1\ i_2}$ defined in (70), as shown at the bottom of the next page. Let P_{e}^n denote the decoding error probability at receiver y_1^1. For we P_e^n we have the expansion in (71), as shown at the bottom of the next page.

Next, we establish the conditions required to ensure that the terms (a) to (i) in the upper bound in (71) approach zero as the block length n approaches infinity. Note that (a) tends to zero as the block length n tends to infinity from the joint asymptotic equipartition property (AEP) of the selected codewords. For simplicity, we list the rate bounds corresponding to y_1^1, and the complete rate region is outlined at the end of this appendix. In the following equations, we use ϕ to denote the empty set.

$$R\left(U_1^1\right) \le r_1^1\left(\phi, \phi\right), \tag{72}$$

$$R\left(V_2^1\right) + R\left(U_1^1\right) \le r_1^1\left(\phi, V_2^1\right), \tag{73}$$

$$R\left(V_1^1\right) + R\left(U_1^1\right) \le r_1^1\left(V_1^1, \phi\right), \tag{74}$$

$$R\left(V_1^2\right) + R\left(U_1^1\right) \le r_1^1\left(V_1^2, \phi\right), \tag{75}$$

$$R\left(V_1^3\right) + R\left(U_1^1\right) \le r_1^1\left(V_1^3, \phi\right), \tag{76}$$

$$R\left(V_2^1\right) + R\left(V_1^3\right) + R\left(U_1^1\right) \le r_1^1\left(V_1^3, V_2^1\right), \tag{77}$$

$$R\left(V_1^2\right) + R\left(V_1^3\right) + R\left(U_1^1\right) \le r_1^1\left(\{V_1^3, V_1^2\}, \phi\right), \tag{78}$$

$$R\left(V_1^1\right) + R\left(V_1^3\right) + R\left(U_1^1\right) \le r_1^1\left(\{V_1^3, V_1^1\}, \phi\right) \tag{79}$$

$$R\left(V_2^1\right) + R\left(V_1^2\right) + R\left(U_1^1\right) \le r_1^1\left(V_1^2, V_2^1\right), \tag{80}$$

$$R\left(V_1^1\right) + R\left(V_1^2\right) + R\left(U_1^1\right) \le r_1^1\left(\{V_1^1, V_1^2\}, \phi\right), \tag{81}$$

$$R\left(V_2^1\right) + R\left(V_1^1\right) + R\left(U_1^1\right) \le r_1^1\left(V_1^1, V_2^1\right), \tag{82}$$

$$R\left(V_2^1\right) + R\left(V_1^2\right) + R\left(V_1^3\right) + R\left(U_1^1\right) \tag{83}$$

$$\le r_1^1\left(\{V_1^3, V_1^2\}, V_2^1\right), \tag{84}$$

$$R\left(V_2^1\right) + R\left(V_1^2\right) + R\left(V_1^1\right) + R\left(U_1^1\right) \tag{85}$$

$$\le r_1^1\left(\{V_1^2, V_1^2\}, V_2^1\right), \tag{86}$$

$$R\left(V_2^1\right) + R\left(V_1^3\right) + R\left(V_1^1\right) + R\left(U_1^1\right) \tag{87}$$

$$\le r_1^1\left(\{V_1^3, V_1^1\}, V_2^1\right), \tag{88}$$

$$R\left(V_1^3\right) + R\left(V_1^2\right) + R\left(V_1^1\right) + R\left(U_1^1\right) \tag{89}$$

$$\le r_1^1\left(\{V_1^3, V_1^2, V_1^1\}, \phi\right), \tag{90}$$

$$R\left(V_2^1\right) + R\left(V_1^1\right) + R\left(V_1^2\right) + R\left(V_1^3\right) + R\left(U_1^1\right)$$

$$\le r_1^1\left(\{V_1^3, V_1^2, V_1^1\}, V_2^1\right). \tag{91}$$

Authorized licensed use limited to: The Libraries at Rensselaer Polytechnic Institute. Downloaded on September 12,2022 at 21:48:32 UTC from IEEE Xplore. Restrictions apply.

APPENDIX III
PROOF OF THEOREM 3

In the standard symmetric Gaussian interference channel we have $a_1 = a_2 = a$, where $a \in \{\beta_1, \beta_2, \beta_3\}$. We denote the sum-rate capacity when channel is $a = \beta_i$ by $C_{\text{sum}}(\beta_i)$. Note that channel states $a \in \{\beta_2, \beta_3\}$ represent a strong Gaussian interference channel, for which the sum-capacity is known, and is given by [7]

$$C_{\text{sum}}(\beta_i) \triangleq= \frac{1}{2}\log\left(1+P+\beta_i P\right). \tag{92}$$

On the other hand, channel $a = \beta_1$ represents a weak Gaussian interference channel, for which the capacity, in general, is unknown. Nevertheless, a simple HK and power allocation scheme presented in [5] achieves a sum-rate within 2 bits of the sum-rate capacity. This sum-rate is given in (93), as shown at the bottom of the next page. (see [5]). Hence, the average sum-rate capacity, when the transmitters have full CSI, is upper bounded as follows

$$\bar{C}_{\text{sum}} \le q^1\left[R^{\text{HK}}_{\text{sum}}(\beta_1)+2\right] + \sum_{s=2}^{3} q^s C_{\text{sum}}(\beta_i). \tag{94}$$

Subsequently, by noting (94) the gap between our sum-rate and sum-rate capacity satisfies

$$\begin{aligned}\Delta &= \bar{C}_{\text{sum}} - \bar{R}_{\text{sum}} \\ &\le q^1\left[R^{\text{HK}}_{\text{sum}}(\beta_1)+2\right] + \sum_{s=2}^{3} q^s C_{\text{sum}}(\beta_i) - \bar{R}_{\text{sum}}.\end{aligned} \tag{95}$$

Next, we find a lower bound on $\bar{R}_{\text{sum}}$, which in conjunction with (95) provides upper bounds on Δ. For this purpose, we consider two different regimes for power P, where in each region, we select a particular power allocation scheme that facilitates finding tractable average sum-rates.

Power region G_1: Power region G_1 is defined as

$$\mathrm{G}_1 \triangleq (0,\beta_3) \cup \left(\beta_3(\beta_3^2+\beta_3-1), +\infty\right). \tag{96}$$

Under this region, we have

$$R^{\text{HK}}_{\text{sum}}(\beta_1) = \frac{1}{2}\log\left(1+P+P\beta_1\right) + \frac{1}{2}\log(2+\beta) - 1. \tag{97}$$

Furthermore, we consider the following power allocation schemes for the transmitters:

$$\text{transmitter 1:} \gamma(V_1^1) = 1. \tag{98}$$

$$\text{transmitter 2:} \gamma(U_2^1) + \gamma(V_2^2) + \gamma(V_2^3) = 1. \tag{99}$$

Under these allocations, the non-zero rates are

$$R_2^1(V_1^1) = \frac{1}{2}\log\left(\frac{1+P+\beta_1 P}{1+P}\right), \tag{100}$$

$$R_2^1(V_2^2) = \frac{1}{2}\log\left(\frac{1+P}{1+(1-\gamma(V_2^2))P}\right), \tag{101}$$

$$R_2^1(V_2^3) = \frac{1}{2}\log\left(\frac{1+(1-\gamma(V_2^2))P}{1+(1-\gamma(V_2^2)-\gamma(V_2^3))P}\right), \tag{102}$$

$$R_2^1(U_2^1) = \frac{1}{2}\log\left(1+(1-\gamma(V_2^2)-\gamma(V_2^3))P\right). \tag{103}$$

Note that the rates in (100)-(103) are the same for all channel states $a = \beta_1$, $a = \beta_2$, or $a = \beta_3$. Hence, by defining $\bar{R}_{\text{sum}}(\mathrm{G}_1)$ as the average sum-rate under this region and power allocation scheme, we have

$$\bar{R}_{\text{sum}}(\mathrm{G}_1) = \frac{1}{2}\log(1+P+\beta_1 P). \tag{104}$$

By noting that $\bar{R}_{\text{sum}}(\mathrm{G}_1) \le \bar{R}_{\text{sum}}$, from (95) we have

$$\Delta(\mathrm{G}_1) \le \sum_{s=1}^{3} q^s \Delta_s(\mathrm{G}_1), \tag{105}$$

where we have defined

$$\Delta_1(\mathrm{G}_1) \triangleq R^{\text{HK}}_{\text{sum}}(\beta_1)+2-\bar{R}_{\text{sum}}(\mathrm{G}_1) = \frac{1}{2}\log(2+\beta_3)+1, \tag{106}$$

$$\Delta_2(\mathrm{G}_1) \triangleq C_{\text{sum}}(\beta_2)-\bar{R}_{\text{sum}}(\mathrm{G}_1) = \frac{1}{2}\log\left(\frac{1+P+\beta_2 P}{1+P+\beta_1 P}\right), \tag{107}$$

$$\left\{V_i^{(n)}(j_i), V_i^{2(n)}(k_i), V_i^{3(n)}(\ell_i), U_i^{1(n)}(j_i,k_i,\ell_i,m_i), U_i^{2(n)}(j_i,k_i,\ell_i,n_i), U_i^{3(n)}(j_i,k_i,\ell_i,x_i)\right\} \tag{66}$$

$$\left(Q^{(n)}, V_1^{1(n)}(\hat{j}_1), V_1^{2(n)}(\hat{k}_1), V_1^{3(n)}(\hat{\ell}_1), U_1^{1(n)}(\hat{j}_1,\hat{k}_1,\hat{\ell}_1,\hat{m}_1), V_2^{1(n)}(\hat{j}_2), y_1^{1(n)}\right) \in A_\epsilon^{(n)}(Q, V_1^1, V_1^2, V_1^3, U_1^1, V_2^1, y_1^1). \tag{67}$$

$$\left(Q^{(n)}, V_1^{1(n)}(\hat{j}_1), V_1^{2(n)}(\hat{k}_1), V_1^{3(n)}(\hat{\ell}_1), U_1^{2(n)}(\hat{j}_1,\hat{k}_1,\hat{\ell}_1,\hat{n}_1), V_2^{1(n)}(\hat{j}_2), V_2^{2(n)}(\hat{k}_2), y_1^{2(n)}\right) \in A_\epsilon^{n}(Q, V_1^1, V_1^2, V_1^3, U_1^2, V_2^1, V_2^2, y_1^2). \tag{68}$$

$$\begin{aligned}&\left(Q^{(n)}, V_1^{1(n)}(\hat{j}_1), V_1^{2(n)}(\hat{k}_1), V_1^{3(n)}(\hat{\ell}_1), U_1^{3(n)}(\hat{j}_1,\hat{k}_1,\hat{\ell}_1,\hat{x}_1), V_2^{1(n)}(\hat{j}_2), V_2^{2(n)}(\hat{k}_2), V_2^{3(n)}(\hat{\ell}_2), y_1^{3(n)}\right) \\ &\qquad \in A_\epsilon^{n}(Q, V_1^1, V_1^2, V_1^3, U_1^3, V_2^1, V_2^2, V_2^3, y_1^3).\end{aligned} \tag{69}$$

$$E_{i_1\ j_1\ k_1\ell_1\ i_2} \triangleq \left\{Q^{(n)}, V_1^{1(n)}(i_1), V_1^{2(n)}(i_1,j_1), V_1^{3(n)}(i_1,j_1,k_1), U_1^{1(n)}(i_1,j_1,k_1,\ell_1), V_2^{1(n)}(i_2), y_1^{1(n)} \in A_\epsilon^{(n)}(Q, V_1^1, V_1^2, V_1^3, U_1^1, V_2^1, y_1^1)\right\}. \tag{70}$$

$$\begin{aligned}P_{\text{e}}^n &= \mathbb{P}\left((\cup_{i_2} E_{1111i_2})^c \bigcup \cup_{(i_1,j_1,k_1,\ell_1)\neq(1,1,1,1)} E_{i_1 j_1 k_1 \ell_1\ i_2}\right) \\ &\le \underbrace{\mathbb{P}((\cup_{i_2} E_{1111i_2})^c)}_{(a)} + \underbrace{\sum_{\ell_1\neq 1}\mathbb{P}(E_{111\ell_1 1})}_{(b)} + \underbrace{\sum_{\ell_1\neq 1, i_2\neq 1}\mathbb{P}(E_{111\ell_1\ i_2})}_{(c)} + \underbrace{\sum_{k_1\neq 1,\ell_1}\mathbb{P}(E_{11k_1\ell_1 1})}_{(d)} + \underbrace{\sum_{k_1\neq 1,\ell_1, i_2\neq 1}\mathbb{P}(E_{11k_1\ell_1\ i_2})}_{(e)} + \underbrace{\sum_{j_1\neq 1,k_1,\ell_1}\mathbb{P}(E_{1jk\ell 1})}_{(f)} \\ &+ \underbrace{\sum_{j_1\neq 1,k_1,\ell_1,i_2\neq 1}\mathbb{P}(E_{1j_1\ k_1\ell_1 1\ i_2})}_{(g)} + \underbrace{\sum_{i_1\neq 1,j_1,k_1,\ell_1}\mathbb{P}(E_{i_1\ j_1\ k_1\ell_1 1})}_{(h)} + \underbrace{\sum_{j_1\neq 1,k_1,\ell_1,i_2\neq 1}\mathbb{P}(E_{i_1 j_1 k_1\ell_1 i_2})}_{(i_1)}.\end{aligned} \tag{71}$$

Authorized licensed use limited to: The Libraries at Rensselaer Polytechnic Institute. Downloaded on September 12,2022 at 21:48:32 UTC from IEEE Xplore. Restrictions apply.

$$R_{\text{sum}}^{\text{HK}}(\beta_1) \triangleq \min\left\{\frac{1}{2}\log(1+P+\beta_1 P)+\frac{1}{2}\log(2+\beta_3)-1, \log(1+\beta_1 P+\beta_3)-1\right\}. \tag{93}$$

$$\Delta_3(\mathrm{G}_1) \triangleq C_{\text{sum}}(\beta_3) - \bar{R}_{\text{sum}}(\mathrm{G}_1) = \frac{1}{2}\log\left(\frac{1+P+\beta_3 P}{1+P+\beta_1 P}\right). \tag{108}$$

Hence, the average sum-rate gap denoted by $\Delta(\mathrm{G}_1)$ is upper bounded by

$$\Delta(\mathrm{G}_1) \overset{(105)}{\leq} \frac{q^1}{2}\log(2+\beta_3) + q^1 + \frac{q^2}{2}\log\left(\frac{1+P+\beta_2 P}{1+P+\beta_1 P}\right) + \frac{q^3}{2}\log\left(\frac{1+P+\beta_3 P}{1+P+\beta_1 P}\right). \tag{109}$$

In the symmetric case of $q^1 = q^2 = q^3 = \frac{1}{3}$, by noting that $\beta = \beta_3 = \frac{1}{\beta_1}$ and $\beta \geq 1$ we obtain

$$\begin{aligned}\Delta(\mathrm{G}_1) &\leq \frac{1}{3}\left[1+\frac{1}{2}\log\left(\frac{1+P(1+\beta)}{1+P(1+\frac{1}{\beta})}\right) + \frac{1}{2}\log\left(\frac{1+2P}{1+P(1+\frac{1}{\beta})}\right)+\frac{1}{2}\log(2+\beta)\right] \\ &\leq \frac{1}{3}\left[1+\log\left(\frac{1+P(1+\beta)}{1+P(1+\frac{1}{\beta})}\right)+\frac{1}{2}\log(2+\beta)\right].\end{aligned} \tag{110}$$

Power region G_2: Power region G_2 is defined as

$$\mathrm{G}_2 \triangleq \left[\beta_3, \beta_3(\beta_3^2+\beta_3-1)\right]. \tag{111}$$

In this region, we have

$$R_{\text{sum}}^{\text{HK}}(\beta_1) = \log(1+\beta_1 P+\beta_3) - 1. \tag{112}$$

Furthermore, in this region, we consider a symmetric power allocation between the two users such that we have

$$\gamma(V_1^1) = \gamma(V_2^1) = 1 - \frac{1}{\beta_1 P} \tag{113}$$

$$\gamma(V_1^2) = \gamma(V_2^2) = \frac{1}{P}\left(\frac{1}{\beta_1}-1\right), \tag{114}$$

$$\gamma(V_1^3) = \gamma(V_2^3) = \frac{1}{P}\left(1-\frac{1}{\beta_3}\right), \tag{115}$$

$$\gamma(U_1^2)+\gamma(U_1^3) = \gamma(U_2^2)+\gamma(U_2^3) = \frac{\beta_1^2}{P}, \tag{116}$$

$$\gamma(U_1^3) = \gamma(U_2^3) = \frac{\beta_1^3}{P}. \tag{117}$$

By adopting this power allocation, the non-zero rates are

$$R_2^1(V_1^1) = R_1^1(V_2^1) = \frac{1}{2}\log\left(\frac{1+\beta_3+\beta_1 P}{2+\beta_3}\right), \tag{118}$$

$$R_1^2(V_1^2) = R_2^2(V_2^2) = \frac{1}{2}\log\left(\frac{1+2\beta_3}{2+\beta_3}\right), \tag{119}$$

$$R_1^3(V_1^3) = R_1^3(V_1^3) = \frac{1}{2}\log\left(\frac{3}{2+\beta_1}\right), \tag{120}$$

$$R_1^3(U_1^1) = R_1^3(U_1^1) = \frac{1}{2}\log\left(\frac{2+\beta_1}{2+\beta_1^2}\right), \tag{121}$$

$$R_2^3(U_1^2) = R_2^3(U_2^2) = \frac{1}{2}\log\left(\frac{2+\beta_1^2}{2+\beta_1^3}\right), \tag{122}$$

$$R_2^3(U_1^3) = R_2^3(U_2^3) = \frac{1}{2}\log\left(\frac{3+\beta_1^3}{2}\right). \tag{123}$$

Hence, the average sum-rate, in this region, denoted by $\bar{R}_{\text{sum}}(\mathrm{G}_2)$ is given by

$$\bar{R}_{\text{sum}}(\mathrm{G}_2) = \log\left(\frac{1+\beta_3+\beta_1 P}{2+\beta_3}\right) + \log\left(\frac{1+2\beta_3}{2+\beta_3}\right) \tag{124}$$

$$+ q_1\log\left(\frac{3}{2+\beta_1^2}\right) + q_2\log\left(\frac{3}{2+\beta_1^3}\right) + q_3\log\left(\frac{3}{2}\right). \tag{125}$$

By noting that $\bar{R}_{\text{sum}}(\mathrm{G}_2) \leq \bar{R}_{\text{sum}}$, from (105) we have

$$\Delta(\mathrm{G}_2) \leq \sum_{s=1}^{3} q^3 \Delta_s(\mathrm{G}_2), \tag{126}$$

where we have defined

$$\begin{aligned}\Delta_1(\mathrm{G}_2) &\triangleq R_{\text{sum}}^{\text{HK}}(\beta_1) + 2 - \bar{R}_{\text{sum}}(\mathrm{G}_2) \\ &= \log(1+\beta_1 P+\beta_3) + 1 - \log\left(\frac{1+\beta_3+\beta_1 P}{2+\beta_3}\right) \\ &\quad - \log\left(\frac{1+2\beta_3}{2+\beta_3}\right) - \log\left(\frac{3}{2+\beta_1^2}\right) \\ &= \log\left(\frac{(2+\beta_1^2)(2+\beta_3)^2}{3(1+2\beta_3)}\right)+1,\end{aligned} \tag{127}$$

$$\begin{aligned}\Delta_2(\mathrm{G}_2) &\triangleq C_{\text{sum}}(\beta_2) - \bar{R}_{\text{sum}}(\mathrm{G}_2) \\ &= \log\left(\frac{\sqrt{1+2P}}{1+\beta_3+\beta_1 P}\right) \\ &\quad + \log\left(\frac{(2+\beta_1^3)(2+\beta_3)^2}{3(1+2\beta_3)}\right),\end{aligned} \tag{128}$$

$$\begin{aligned}\Delta_3(\mathrm{G}_2) &\triangleq C_{\text{sum}}(\beta_3) - \bar{R}_{\text{sum}}(\mathrm{G}_2) \\ &= \log\left(\frac{\sqrt{1+P+\beta_3 P}}{1+\beta_3+\beta_1 P}\right) \\ &\quad + \log\left(\frac{2(2+\beta_3)^2}{3(1+2\beta_3)}\right).\end{aligned} \tag{129}$$

Hence, the average sum-rate, denoted by $\Delta(\mathrm{G}_2)$ in symmetric case of $q^1 = q^2 = q^3 = \frac{1}{3}$, is readily upper bounded by

$$\Delta(\mathrm{G}_2) \leq \frac{1}{3}\left[\log\frac{4}{3} + \log\left(\frac{1+P(1+\beta)}{1+P/\beta+\beta}\right) + 3\log\frac{(2+\beta)^2}{1+2\beta}\right], \tag{130}$$

where we have leveraged that $P \geq \beta$ and $\beta \geq 1$ to simplify some terms.

REFERENCES

[1] V. R. Cadambe and S. A. Jafar, "Interference alignment and degrees of freedom of the K-user interference channel," *IEEE Trans. Inf. Theory*, vol. 54, no. 8, pp. 3425–3441, Jul. 2008.

Authorized licensed use limited to: The Libraries at Rensselaer Polytechnic Institute. Downloaded on September 12,2022 at 21:48:32 UTC from IEEE Xplore. Restrictions apply.

[2] M. A. Maddah-Ali, A. S. Motahari, and A. K. Khandani, "Communication over MIMO X channels: Interference alignment, decomposition, and performance analysis," *IEEE Trans. Inf. Theory*, vol. 54, no. 8, pp. 3457–3470, Aug. 2008.

[3] T. Han and K. Kobayashi, "A new achievable rate region for the interference channel," *IEEE Trans. Inf. Theory*, vol. IT-27, no. 1, pp. 49–60, Jan. 1981.

[4] H.-F. Chong, M. Motani, H. K. Garg, and H. El Gamal, "On the Han–Kobayashi region for the interference channel," *IEEE Trans. Inf. Theory*, vol. 54, no. 7, pp. 3188–3195, Jun. 2008.

[5] R. H. Etkin, N. David, and H. Wang, "Gaussian interference channel capacity to within one bit," *IEEE Trans. Inf. Theory*, vol. 54, no. 12, pp. 5534–5562, Dec. 2008.

[6] A. Carleial, "A case where interference does not reduce capacity," *IEEE Trans. Inf. Theory*, vol. IT-21, no. 5, pp. 569–570, Sep. 1975.

[7] H. Sato, "The capacity of the Gaussian interference channel under strong interference," *IEEE Trans. Inf. Theory*, vol. IT-27, no. 6, pp. 786–788, Nov. 1981.

[8] R. Benzel, "The capacity region of a class of discrete additive degraded interference channels," *IEEE Trans. Inf. Theory*, vol. IT-25, no. 2, pp. 228–231, Mar. 1979.

[9] A. Gamal and M. Costa, "The capacity region of a class of deterministic interference channels," *IEEE Trans. Inf. Theory*, vol. IT-28, no. 2, pp. 343–346, Mar. 1982.

[10] V. R. Cadambe, S. A. Jafar, and S. Vishwanath, "The capacity region of a class of deterministic Z-channels," in *Proc. IEEE Int. Symp. Inf. Theory*, Seoul, South Korea, Jun. 2009, pp. 2634–2638.

[11] H.-F. Chong, M. Motani, and H. K. Garg, "The capacity region of a class of interference channels," in *Proc. IEEE Int. Symp. Inf. Theory*, Nice, France, Jun. 2007, pp. 2856–2860.

[12] G. Bresler and D. Tse, "The two-user Gaussian interference channel: A deterministic view," *Eur. Trans. Telecommun.*, vol. 19, no. 4, pp. 333–354, Apr. 2008.

[13] L. Wang, E. Sasoglu, and Y.-H. Kim, "Sliding-window superposition coding for interference networks," in *Proc. IEEE Int. Symp. Inf. Theory*, Honolulu, HI, USA, Jun. 2014, pp. 2749–2753.

[14] B. Bandemer, A. El Gamal, and Y.-H. Kim, "Optimal achievable rates for interference networks with random codes," *IEEE Trans. Inf. Theory*, vol. 61, no. 12, pp. 6536–6549, Dec. 2015.

[15] H. D. Tuan, H. H. M. Tam, H. H. Nguyen, T. Q. Duong, and H. V. Poor, "Superposition signaling in broadcast interference networks," *IEEE Trans. Commun.*, vol. 65, no. 11, pp. 4646–4656, Nov. 2017.

[16] H. Yagi and H. V. Poor, "Multi-level rate-splitting for synchronous and asynchronous interference channels," in *Proc. Int. Symp. Inf. Theory*, St. Petersburg, Russia, Jul. 2011, pp. 2080–2084.

[17] Y. Zhao, C. W. Tan, A. S. Avestimehr, S. N. Diggavi, and G. J. Pottie, "On the maximum achievable sum-rate with successive decoding in interference channels," *IEEE Trans. Inf. Theory*, vol. 58, no. 6, pp. 3798–3820, Jun. 2012.

[18] C. Geng, N. Naderializadeh, A. S. Avestimehr, and S. A. Jafar, "On the optimality of treating interference as noise," *IEEE Trans. Inf. Theory*, vol. 61, no. 4, pp. 1753–1767, Apr. 2015.

[19] M. Ashraphijuo, A. Tajer, C. Gong, and X. Wang, "A receiver-centric approach to interference management: Fairness and outage optimization," *IEEE Trans. Inf. Theory*, vol. 62, no. 10, pp. 5619–5642, Oct. 2016.

[20] X. Yi and H. Sun, "Opportunistic treating interference as noise," *IEEE Trans. Inf. Theory*, vol. 66, no. 1, pp. 520–533, Jan. 2020.

[21] C. Huang, S. A. Jafar, S. Shamai (Shitz), and S. Vishwanath, "On degrees of freedom region of MIMO networks without channel state information at transmitters," *IEEE Trans. Inf. Theory*, vol. 58, no. 2, pp. 849–857, Feb. 2012.

[22] Y. Zhu and D. Guo, "The degrees of freedom of isotropic MIMO interference channels without state information at the transmitters," *IEEE Trans. Inf. Theory*, vol. 58, no. 1, pp. 341–352, Jan. 2012.

[23] C. S. Vaze and M. K. Varanasi, "The degree-of-freedom regions of MIMO broadcast, interference, and cognitive radio channels with no CSIT," *IEEE Trans. Inf. Theory*, vol. 58, no. 8, pp. 5354–5374, Aug. 2012.

[24] T. Gou, S. A. Jafar, and C. Wang, "On the degrees of freedom of finite state compound wireless networks," *IEEE Trans. Inf. Theory*, vol. 57, no. 6, pp. 3286–3308, Jun. 2011.

[25] W. Shin, B. Lee, B. Shim, and J. Lee, "A MIMO relay with delayed feedback can improve DoF in K-user MISO interference channel with no CSIT," *IEEE Trans. Veh. Technol.*, vol. 65, no. 12, pp. 10188–10192, Dec. 2016.

[26] Y.-S. Jeon, N. Lee, and R. Tandon, "Degrees of freedom and achievable rate of wide-band multi-cell multiple access channels with no CSIT," *IEEE Trans. Commun.*, vol. 66, no. 4, pp. 1772–1786, Apr. 2017.

[27] M. Morales-Cespedes, L. Vandendorpe, and A. G. Armada, "Degrees of freedom of 2-tier networks without channel state information at the transmitter," *IEEE Signal Process. Lett.*, vol. 26, no. 2, pp. 382–386, Feb. 2019.

[28] C. Geng and S. A. Jafar, "On the optimality of treating interference as noise: Compound interference networks," *IEEE Trans. Inf. Theory*, vol. 62, no. 8, pp. 4630–4653, Aug. 2016.

[29] S. A. Jafar, "Blind interference alignment," *IEEE J. Sel. Topics Signal Process.*, vol. 6, no. 3, pp. 216–227, Jun. 2012.

[30] Y. Lu and W. Zhang, "Blind interference alignment in the K-user MISO interference channel," in *Proc. Global Commun. Conf.*, Atlanta, GA, USA, Jun. 2013, pp. 3464–3469.

[31] Y. Lu, W. Zhang, and K. B. Letaief, "Blind interference alignment with diversity in K-user interference channels," *IEEE Trans. Commun.*, vol. 62, no. 8, pp. 2850–2859, Aug. 2014.

[32] S. A. Jafar, "Exploiting channel correlations-simple interference alignment schemes with no CSIT," in *Proc. IEEE Global Telecommun. Conf.*, Miami, FL, USA, Dec. 2010, pp. 1–5.

[33] T. Gou, C. Wang, and S. A. Jafar, "Aiming perfectly in the dark-blind interference alignment through staggered antenna switching," *IEEE Trans. Signal Process.*, vol. 59, no. 6, pp. 2734–2744, Jun. 2011.

[34] C. Wang, H. C. Papadopoulos, S. A. Ramprashad, and G. Caire, "Improved blind interference alignment in a cellular environment using power allocation and cell-based clusters," in *Proc. IEEE Int. Conf. Commun.*, Kyoto, Japan, Jun. 2011, pp. 1–6.

[35] S. Akoum, C. S. Chen, M. Debbah, and R. W. Heath, Jr., "Data sharing coordination and blind interference alignment for cellular networks," in *Proc. IEEE Global Commun. Conf.*, Anaheim, CA, USA, Dec. 2012, pp. 4273–4277.

[36] C. Wang, "Degrees of freedom characterization: The 3-user SISO interference channel with blind interference alignment," *IEEE Commun. Lett.*, vol. 18, no. 5, pp. 757–760, May 2014.

[37] D. Castanheira, A. Silva, and A. Gameiro, "Retrospective interference alignment: Degrees of freedom scaling with distributed transmitters," *IEEE Trans. Inf. Theory*, vol. 63, no. 3, pp. 1721–1730, Mar. 2017.

[38] X. Chen *et al.*, "Blind interference alignment in two-cell Z interference MIMO channel," *IEEE Access*, vol. 5, pp. 10526–10532, Jun. 2017.

[39] M. Johnny and A. Vahid, "Exploiting coherence time variations for opportunistic blind interference alignment," *IEEE Trans. Commun.*, early access, 2020, doi: 10.1109/TCOMM.2020.3011687.

[40] S. A. Jafar, "Topological interference management through index coding," *IEEE Trans. Inf. Theory*, vol. 60, no. 1, pp. 529–568, Jan. 2014.

[41] N. Naderializadeh and A. S. Avestimehr, "Interference networks with no CSIT: Impact of topology," *IEEE Trans. Inf. Theory*, vol. 61, no. 2, pp. 917–938, Feb. 2015.

[42] M. Morales-Cespedes, J. Plata-Chaves, D. Toumpakaris, S. A. Jafar, and A. Garcia Armada, "Blind interference alignment for cellular networks," *IEEE Trans. Signal Process.*, vol. 63, no. 1, pp. 41–56, Jan. 2015.

[43] H. Yang, W. Shin, and J. Lee, "Degrees of freedom for K-user SISO interference channels with blind interference alignment," in *Proc. Asilomar Conf. Signals, Syst. Comput.*, Pacific Grove, CA, Feb. 2015, pp. 1097–1101.

[44] S. Akhlaghi and M. Baghani, "On the average achievable rate of block fading decentralized interference channel," *IEEE Commun. Lett.*, vol. 15, no. 9, pp. 992–994, Sep. 2011.

[45] A. Vahid, M. A. Maddah-Ali, A. S. Avestimehr, and Y. Zhu, "Binary fading interference channel with no CSIT," *IEEE Trans. Inf. Theory*, vol. 63, no. 6, pp. 3565–3578, Jun. 2017.

[46] Y. Zhu and C. Shen, "On layered erasure interference channels without CSI at transmitters," in *Proc. IEEE Int. Symp. Inf. Theory*, Barcelona, Spain, Jul. 2016, pp. 710–714.

[47] A. Raja, V. M. Prabhakaran, and P. Viswanath, "The two-user compound interference channel," *IEEE Trans. Inf. Theory*, vol. 55, no. 11, pp. 5100–5120, Nov. 2009.

[48] Y. Zhu and D. Guo, "Ergodic fading Z-interference channels without state information at transmitters," *IEEE Trans. Inf. Theory*, vol. 57, no. 5, pp. 2627–2647, May 2011.

[49] P.-H. Lin, E. A. Jorswieck, and R. F. Schaefer, "On ergodic fading Gaussian interference channels with statistical CSIT," in *Proc. IEEE Inf. Theory Workshop*, Cambridge, U.K., Sep. 2016, pp. 454–458.

Authorized licensed use limited to: The Libraries at Rensselaer Polytechnic Institute. Downloaded on September 12,2022 at 21:48:32 UTC from IEEE Xplore. Restrictions apply.

[50] P.-H. Lin, E. A. Jorswieck, C. R. Janda, M. Mittelbach, and R. F. Schaefer, "On stochastic orders and fading Gaussian multi-user channels with statistical CSIT," in *Proc. IEEE Int. Symp. Inf. Theory*, Paris, France, Jun. 2019, pp. 1497–1501.

[51] J. Sebastian, C. Karakus, S. Diggavi, and I.-H. Wang, "Rate splitting is approximately optimal for fading Gaussian interference channels," in *Proc. Allerton Conf. Commun., Control, Comput.*, Monticello, IL, Sep. 2015, pp. 315–321.

[52] J. Sebastian, C. Karakus, and S. Diggavi, "Approximate capacity of fast fading interference channels with no instantaneous CSIT," *IEEE Trans. Commun.*, vol. 66, no. 12, pp. 6015–6027, Dec. 2018.

[53] T. Cover, "Broadcast channels," *IEEE Trans. Inf. Theory*, vol. IT-18, no. 1, pp. 2–14, Jan. 1972.

[54] S. Shamai (Shitz), "A broadcast strategy for the Gaussian slowly fading channel," in *Proc. IEEE Int. Symp. Inf. Theory*, Ulm, Germany, Jun. 1997, p. 150.

[55] S. Shamai (Shitz) and A. Steiner, "A broadcast approach for a single-user slowly fading MIMO channel," *IEEE Trans. Inf. Theory*, vol. 49, no. 10, pp. 2617–2635, Oct. 2003.

[56] C. Shen, T. Liu, and M. P. Fitz, "On the average rate performance of hybrid-ARQ in quasi-static fading channels," *IEEE Trans. Commun.*, vol. 57, no. 11, pp. 3339–3352, Nov. 2009.

[57] C. Gong, O. Abu-Ella, A. Tajer, and X. Wang, "Constrained group decoder for interference channels," *J. Commun., Special Issue Future Directions Comput. Netw.*, vol. 7, no. 5, pp. 382–390, May 2012.

[58] T. T. Kim and M. Skoglund, "On the expected rate of slowly fading channels with quantized side information," *IEEE Trans. Commun.*, vol. 55, no. 4, pp. 820–829, Apr. 2007.

[59] Y. Liu, K. N. Lau, O. Y. Takeshita, and M. P. Fitz, "Optimal rate allocation for superposition coding in quasi-static fading channels," in *Proc. IEEE Int. Symp. Inf. Theory*, Lausanne, Switzerland, Jun. 2002, p. 111.

[60] X. Wang and M. T. Orchard, "Design of superposition coded modulation for unequal error protection," in *Proc. IEEE Int. Conf. Commun.*, Helsinki, Finland, Jun. 2001, pp. 412–416.

[61] S. Shamai (Shitz), "A broadcast approach for the multiple-access slow fading channel," in *Proc. IEEE Int. Symp. Inf. Theory*, Sorrento, Italy, Jun. 2000, p. 128.

[62] P. Minero and D. N. C. Tse, "A broadcast approach to multiple access with random states," in *Proc. IEEE Int. Symp. Inf. Theory*, Nice, France, Jun. 2007, pp. 2566–2570.

[63] S. Zou, Y. Liang, and S. Shamai (Shitz), "Multiple access channel with state uncertainty at transmitters," in *Proc. IEEE Int. Symp. Inf. Theory*, Istanbul, Turkey, Jul. 2013, pp. 1466–1470.

[64] S. Kazemi and A. Tajer, "Multiaccess communication via a broadcast approach adapted to the multiuser channel," *IEEE Trans. Commun.*, vol. 66, no. 8, pp. 3341–3353, Aug. 2018.

[65] M. Zohdy, S. Kazemi, and A. Tajer, "A broadcast approach to multiple access with partial CSIT," in *Proc. IEEE Global Commun. Conf.*, Abu Dhabi, United Arab Emirates, Dec. 2018, pp. 1–6.

[66] M. Zohdy, A. Tajer, and S. Shamai (Shitz), "Broadcast approach to multiple access with local CSIT," *IEEE Trans. Commun.*, vol. 67, no. 11, pp. 7483–7498, Nov. 2019.

[67] A. Carleial, "Interference channels," *IEEE Trans. Inf. Theory*, vol. IT-24, no. 1, pp. 60–70, Jan. 1978.

[68] I. Sason, "On achievable rate regions for the Gaussian interference channel," *IEEE Trans. Inf. Theory*, vol. 50, no. 6, pp. 1345–1356, Jun. 2004.

[69] S. A. K. Hoseini and S. Akhlaghi, "The expected achievable distortion of two-user decentralized interference channels," *J. Commun. Eng.*, vol. 5, no. 2, pp. 80–93, 2016.

[70] M. A. Maddah-Ali and U. Niesen, "Cache-aided interference channels," *IEEE Trans. Inf. Theory*, vol. 65, no. 3, pp. 1714–1724, Mar. 2019.

Authorized licensed use limited to: The Libraries at Rensselaer Polytechnic Institute. Downloaded on September 12,2022 at 21:48:32 UTC from IEEE Xplore. Restrictions apply.